Conceptual Design of Tiltrotor Aircraft for Urban Air Mobility

Michael Radotich
NASA Ames Research Center
Moffett Field, CA, USA

ABSTRACT

There has been an abundance of new and novel aircraft designs created for Urban Air Mobility (UAM) in recent years. The National Aeronautics and Space Administration (NASA) contributes to the research and development of this industry in part by applying its aircraft design tools to create conceptual designs of UAM reference vehicles. The vehicles are intended to quantify the tradeoffs and performance capabilities necessary for VTOL (vertical takeoff and landing) aircraft in the UAM design space. The reference vehicles represent a variety of configurations that seek to encompass many of the design characteristics suitable for UAM. This work focuses on the conceptual design process of two new NASA reference vehicles. Both aircraft are configured as conventional tiltrotors, but one is powered by turboshaft engines, and one is fully electric. The sizing and performance of the two aircraft are discussed, as well as how the performance and characteristics compare to a selection of other NASA reference vehicles. It is found that the tiltrotor configuration is capable of reaching speeds 43% to 51% faster than the other turboshaft designs, and 54% to 93% faster than the other electric designs. The increased speed leads to a 24% to 42% decrease in overall mission time.

NOTATION

AAM	Advanced Air Mobility
A_{ref}	Rotor Disk Area
b	Span
CAD	Computer Aided Design
CAMRADII	Comprehensive Analytical Model of Rotorcraft Aerodynamics and Dynamics II
Cd	Coefficient of Drag
C_T	Coefficient of Thrust
D	Drag
D_{climb}	Climb Distance
DGW	Design Gross Weight
DL	Disk Loading
eVTOL	Electric Vertical Take-Off and Landing
FM	Figure of Merit
ft	Feet
ft/s	Feet per Second
GUI	Graphical User Interface
HECTR	High Efficiency Civil Tiltrotor
hp	Horsepower
hr	Hour
kappa	Induced Power Coefficient
kts	Knots
lb	Pound
LCTR	Large Civil Tiltrotor
min	Minute
MJ	Megajoules
NACA	National Advisory Committee for Aeronautics
NASA	National Aeronautics and Space Administration
nblade	Number of Rotor Blades
NDARC	NASA Design and Analysis of Rotorcraft
nm	Nautical Mile
P	Power
P_{climb}	Climb Power
P_{cruise}	Cruise Power
psf	Pounds per Square Foot
q	Dynamic Pressure
S	Area
sec	Second
SFC	Specific Fuel Consumption
sq. ft	Square Feet
T	Thrust
t_{climb}	Climb Time
t_{cruise}	Cruise Time
UAM	Urban Air Mobility
V	Velocity
V_{br}	Best Range Speed
Vtip	Rotor Tip Speed
VTOL	Vertical Take-Off and Landing
V_y	Climb Speed
W	Weight
Wh/kg	Watt-hours per Kilogram
WL	Wing Loading
η	Propulsive Efficiency
μ_z (muz)	Axial Advance Ratio
ρ	Density
σ	Solidity
$_{ht}$	Horizontal Tail
$_{V}$	V-Tail
$_{vt}$	Vertical Tail

INTRODUCTION

Urban Air Mobility (UAM) is the concept of utilizing vertical takeoff and landing (VTOL) aircraft to transport cargo and passengers quickly over short distances in urban areas. In 2016 UBER released a whitepaper titled "Fast-Forwarding to a Future of On-Demand Urban Air Transportation" [1]. The paper describes revolutionizing the urban transportation industry using VTOL aircraft. It aims to add another mode of fast, reliable, and eventually cheap transportation that will provide the masses with newfound mobility, while simultaneously decongesting the current transportation means.

Urban Air Mobility will require close, integrated operation of VTOL aircraft in crowded urban areas. A primary reason extensive urban operation is not yet commonplace is aircraft noise. UAM vehicles must be quiet. Current helicopters do not meet the noise requirements for this level of integration. UAM vehicles will need to be similar in noise to standard cars and trucks. Two primary factors in helicopter noise are engine noise and high rotor tip speeds. UAM designs reflect that need for reduced noise with lower rotor tip speeds, modified rotor geometry, and electric propulsion. Electric propulsion is significantly quieter than turboshaft or diesel engines and eliminates the emissions concerns with increased aircraft presence, though battery technology (particularly battery specific energy) is a significant limiting factor in electric aircraft.

As part of the effort to enable this industry, NASA is contributing a set of reference vehicles to inform technology development. These reference vehicles represent a variety of possible vehicle configurations, and the research for this paper focuses on the conceptual design of one configuration: the tiltrotor.

NASA's advanced air mobility (AAM) project aims to help realize aviation markets in local, regional, interregional, and urban areas. UAM is encompassed by AAM, and the work described in this paper is tailored specifically for the UAM subset of operation, though it may have future implications for UAM as well.

Simultaneous with the push for UAM come advancements in eVTOL (electric vertical takeoff and landing) technology and more companies entering the electric aviation market. Hundreds of companies, established aerospace companies and small startups alike, are designing and building eVTOL aircraft. The Vertical Flight Society tracks these aircraft and keeps a directory of current concepts [2]. These companies are some of the intended benefactors of NASA's work to enable UAM. A goal of NASA's involvement in UAM is giving these companies the tools and knowledge to be successful in creating this new industry.

This paper builds upon prior work in designing reference vehicles for UAM, including [3], [4], and [5]. The design process includes the use of NASA's NDARC aircraft sizing software, CAMRADII comprehensive analysis software, and SOLIDWORKS 3D modeling software to create two tiltrotor aircraft models, one powered by a turboshaft engine and one fully electric, designed specifically for a UAM mission. These aircraft are compared to each other, as well as the other NASA reference vehicle configurations.

BACKGROUND

NASA Reference Models

To support the UAM mission, NASA is designing a set of reference vehicles to evaluate performance and characteristics of different configurations. Part of the effort is technology development and determining where technology needs to be improved to guide research and development, as well as developing the tools to model VTOL and eVTOL aircraft [3]. These reference models are not intended to model any specific company's aircraft or mimic existing vehicles, rather they are intended to be generic designs to provide insight into performance and characteristics of general configurations for UAM, to serve as mechanisms for evaluating technology needs and payoff, and to provide common discussion platforms for public discussion.

Accurate comparison between different types of these vehicles is desired. Because of this, a standard UAM flight mission was developed. The resulting mission is a 6 passenger, 75 nautical mile, two-hop flight [5]. More information is discussed in a following section.

3 other NASA reference vehicles, each designed to the standard mission, will be used as comparison for the tiltrotor. These configurations are the side-by-side helicopter, the quadrotor, and the lift+cruise. Each configuration includes a turboshaft and electric variation.

Side-By-Side

The side-by-side helicopter features a pair of intermeshing rotors that act as a unified lifting and thrusting device in forward flight. The rotors are mounted on the ends of a rotor support crossbar along with the two engines/motors. The rotors are connected through the crossbar with an interconnect shaft that keeps the rotors synchronized as well as providing the ability to send power from one side to the other in the

Presented at the VFS Aeromechanics for Advanced Vertical Flight Technical Meeting, San Jose, CA, Jan 25-27, 2022.

event of in inoperative engine/motor. Figure 1 depicts the turboshaft variation of the side-by-side.

Figure 1. Side-by-side concept vehicle

Quadrotor

The quadrotor has four rotors connected to a main fuselage by four arms in an 'X' configuration. It is powered by two turboshaft engines or four electric motors. It represents multicopter configurations, as the wake of the front rotors interferes with the rear rotors. It was found that raising the rear rotors higher than the front rotors reduces the interference effects and increases the overall efficiency of the vehicle. The rotors are all interconnected via drive shafts to allow for shared power between all rotors in the case of engine/motor failure. The turboshaft version is shown in Figure 2.

Figure 2. Quadrotor concept vehicle

Lift + Cruise

The lift+cruise is the only aircraft discussed that does not have a true turboshaft variation. Distributed electric propulsion is a requirement for the lift+cruise, therefore it was designed to have a turboelectric hybrid and full electric version. The turboelectric includes a turboshaft engine powering a generator to charge a battery that then distributes power to motors driving 8 lifting rotors and a pusher propeller. The aircraft has two distinct operating modes: helicopter and cruise. Helicopter mode flight is powered by eight wing-boom mounted rotors. The pusher propeller engages for transition to forward flight, and once cruise is reached the lifting rotors are stopped and oriented parallel to the airflow to reduce drag. The aircraft then operates as a pusher propeller airplane with the wing providing lift and the pusher providing thrust. The wing can be relatively small since low-speed flight is assisted by the lifting rotors. The turboelectric variant will be grouped with the turboshaft variants of the other vehicles for discussion purposes, as it is the closest this configuration can get to turboshaft power (interconnecting the rotors and propeller with shafts is not considered because of weight and complexity). Figure 3 shows the lift+cruise aircraft.

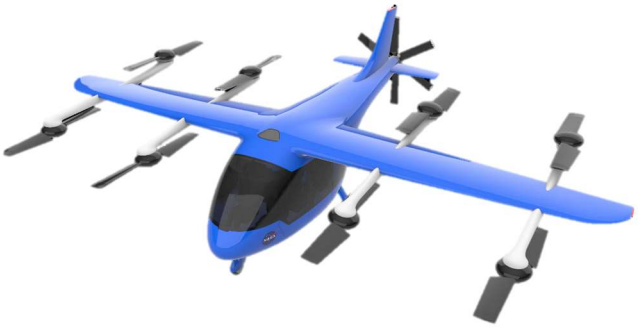

Figure 3. Lift+cruise concept vehicle

Tiltrotors

Tiltrotors are a type of aircraft configuration characterized by the ability to use the lifting rotors as propellers in forward flight by tilting them 90 degrees and obtaining lift from a wing. The general goal is to combine the VTOL capabilities of a helicopter with the forward flight speeds, efficiency, and range of an airplane. When a conventional helicopter is in forward (edgewise) flight, it experiences asymmetric lift, since the effective velocity of the advancing side of the rotor is the rotational speed plus the aircraft speed, and the retreating blade velocity is the rotational speed minus the aircraft speed. If the helicopter gains a high enough velocity, the retreating blade will stall and the resulting lift limit becomes a limit for the advancing blade as well (if roll moment balance is required), imposing an effective speed limit on edgewise flight at around 150 kts. Tiltrotors solve this problem by tilting the rotors forward, changing them from edgewise to axial flight, and generating the lift with a wing, allowing for maximum speeds around 300 kts [6].

While there can be various configurations and number of rotors on a tiltrotor, the standard and most common tiltorotor configuration uses two, wingtip-mounted rotors in a transverse orientation. The most well-known tiltrotor, the V-22 Osprey [6], employs this configuration. The Osprey was developed from NASA's expertimental XV-15 [7]. A characteristic of note is that for these designs the engines are also mounted on the wingtips and rotate with the rotors, this eliminates the neeed for a heavy and complex drive system capable of driving and tilting the rotors. A diagram of the XV-15 is shown in Figure 4 representing the conventional tiltrotor design.

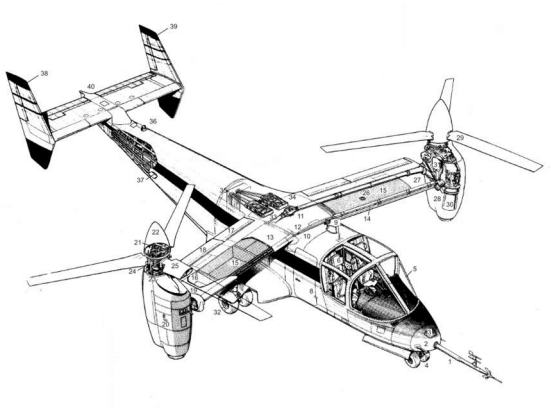

Figure 4. Diagram of the XV-15 tiltrotor [7]

METHODS

NDARC Baseline Model

The design begins in the aircraft system analysis tool NDARC (NASA Design and Analysis of Rotorcraft) [8]. NDARC sizes an aircraft based on design conditions and missions, then analyzes the vehicle's performance. It is a flexible design tool capable of modeling and estimating the performance, weights, and parameters of both standard and unconventional configurations. Suited for a conceptual design environment, the models are low fidelity, but the code allows for the input of parameters from higher fidelity tools to improve the predictions.

An aircraft is built in NDARC as a set of components. Components including fuselage, rotors, wings, tails, and propulsion are defined, and attributes are obtained from the components and summed to the entire aircraft.

When designing a new aircraft in NDARC, it is never advised to start completely from scratch. New designs are built upon a selection of standard designs, or previous designs for aircraft with similar characteristics. The UAM tiltrotor NDARC baseline model is created using two previous aircraft designs for reference. The first is the previously mentioned side-by-side NASA reference vehicle, and the second is the NASA's High Efficiency Civil Tiltrotor (HECTR) design [9].

Components

The sized aircraft model is created by two sets of information: one describing the initial aircraft, and one describing the missions and sizing conditions that generate the sized model, as well as performance missions not used in sizing. In the aircraft description, the individual aircraft components are defined.

Aircraft

The Aircraft component defines general characteristics of the aircraft. The initial gross weight to start the iterations is set to 6,000 lb, higher than desired but in the right order of magnitude. Two rotors, one wing, two tail surfaces, and two of the same engine are defined. Since this is a tiltrotor, a conversion schedule mst be defined. The conversion schedule was informed by the HECTR tiltrotor model and begins transition at 40 knots and fully converts to airplane mode at 110 kts.

Systems

To be consistent with the other NASA reference vehicles, the system weights are based on the side-by-side model, maintaining consistency on passenger and furnishing weights, de-icing equipment, vibration treatment, environmental control, and automatic flight controls. Since the mission is consistent between vehicles, the factors that influence these weights will be similar. The tiltrotor will have increased weight from the addition of fixed wing flight controls and conversion controls.

Fuselage

NASA reference vehicles use a standard, 30-ft long by 6-ft wide by 5.1-ft tall fuselage to carry the six-passenger payload. This standardizes the drag effects of the fuselage and helps keep the vehicle in the desired footprint for VTOL operations in the UAM infrastructure.

Landing Gear

A main factor in landing gear design for NDARC is fixed vs retractable landing gear. The retractable landing gear produces less drag in forward flight but adds weight with a retracting mechanism. Due to the short forward flight segments of the UAM mission, a fixed landing gear was chosen, as the slight increase in cruise efficiency was not worth the weight penalty.

Rotor

The rotor is a complex system, and low fidelity analysis has limited accuracy. For this reason, the initial rotor aerodynamic performance parameters, as well as twist and taper were derived from the HECTR rotor because it provides an acceptable starting point for initial sizing. In-depth rotor analysis is then performed to optimize the rotor in CAMRADII and the NDARC rotor model is adjusted to reflect the CAMRADII higher fidelity results, as discussed in following sections.

The rotor was chosen to be a hingeless rotor based on the findings of NASA's Large Civil Tiltrotor design [10]. Hingeless (stiff) rotors have better stability, but higher loads than articulated (hinged or gimballed) rotors. Additionally, a hingeless rotor is needed to use more than 3 blades. Hingeless rotors tend to be less susceptible to whirl flutter instability, meaning the wing will not need to be as torsionally stiff (or heavy) as it would with a gimballed or articulated rotor.

Wing

For conceptual design, the wing does not depend on specific airfoils. For the baseline model, a wing based on the parameters of the HECTR wing is a good starting point. The tiltrotor wing has a thickness of 20%, as tiltrotors need relatively thick wings due to the large proprotors on the wingtips. The wings are given slight forward sweep and dihedral, 3.8 degrees and 5 degrees respectively. A slight taper ratio of 0.875 is given to the wings.

Tail

The tail is initially modeled in NDARC as a conventional tail. Using guidelines from Raymer's aircraft design book [11], the tail volume ratios of the horizontal and vertical tails were chosen to be 0.7 and 0.04 respectively, with aspect ratios of 3.4 and 2.4. These two parameters for each tail will be used to size the tail. Once NDARC sizes the conventional tail, it is converted into a V-tail as described in the NDARC Theory Manual [12]. The equations are shown below, where S is planform area, δ is the dihedral angle of the V-tail, b is span, and AR is aspect ratio. The subscript denotes vertical tail (vt), horizontal tail (ht), and V-tail (V).

$$S_V = S_{ht} + S_{vt}$$

$$AR_V = AR_{ht}$$

$$\delta = \tan^{-1}\left(\sqrt{\left(\frac{S_{vt}}{S_{ht}}\right)}\right)$$

$$b_V = \sqrt{AR_V S_V} = b_{ht}/\cos(\delta)$$

Propulsion

This model is designed with a two-speed transmission, one gear for hover and one for cruise. Many historical tiltrotors like the XV-15 only reduce their tip speed in cruise to about 80% of hover tip speed [13]. This design reduces the cruise tip speed to 50% of the hover tip speed. The tip speed varies by a speed schedule shown in Figure 5, increasing until 60 kts, then decreasing to 50% at 150 kts. It then increases with airspeed to a maximum of 70%. The tip speed schedule is designed to maximize rotor efficiency for cruise speeds [14].

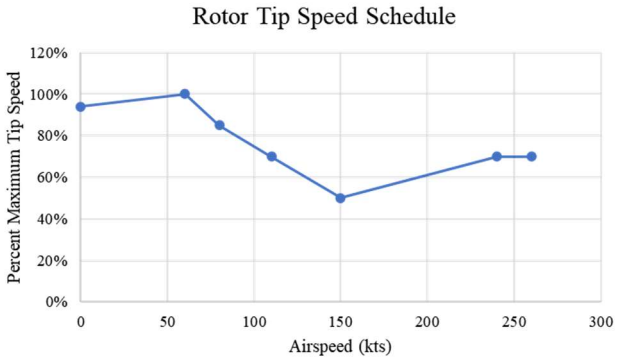

Figure 5. Rotor tip speed schedule

The main gearbox reduces weight by separating the delivery of torque and the thrust and moment reaction. The nacelle structure reacts thrust and moment from the rotors, allowing the main gearbox to be lighter. The advanced drive system technology this is modeled after can be found in [14] and [15].

Engine

The engines used in the turboshaft model are pre-existing state of the art engines included in the standard NDARC distribution. The size of the engine will be scaled as part of the design code, but the parameters are based off the 500-hp model. The weight of the engine in lb for this model scales to be 34% of the engine power in hp, so the engine weight will scale accordingly with power. Specific fuel consumption (sfc) is how much fuel (lb) is burned per hour at maximum continuous power. To be scaleable, sfc is input as lb per horsepower per hour, so that as sized engine power increases so does fuel flow. The sfc for this engine model is 0.54 lb/hp-hr.

Battery

For the electric version, as with the rest of the NASA reference vehicles, advanced technology batteries are used as the energy source. The batteries are modeled with lithium-ion discharge characteristics, but with cell level specific energy of 650 Wh/kg. After accounting for unusuable energy (20%) and installation weight (30%), the installed usable (pack) battery energy is 400 Wh/kg. For comparison, this is significantly higher than current lithium-ion battery energy density of between 150-260 Wh/kg, but represents a future breakthrough in battery technology. Promising battery chemistries for this level of energy density include lithium metal or lithium sulfur [16].

Technology Factors

Weight models in NDARC are based on equations derived from historical aircraft data. To account for advancements in

technology, NDARC implements technology factors. Technology factors allow the designer to make predictions about component weights based on current research and anticipated technological advancements. Light composite materials and improved engine efficiency are examples of technology factors that may be implemented. Creating technology factors is an extensive process involving analyzing current research and determining where commercial technology may be in the near future. For the purposes of this research, the HECTR technology factors were used because they are representative of an advanced technology tiltrotor.

UAM Mission

To provide valid comparison between NASA reference models, they need to be sized to a standard mission. The UAM mission includes two sizing conditions, one sizing mission, and six performance conditions that do not affect sizing, but measure the performance of the sized aircraft. All missions and conditions are flown with a standard 6 passenger payload represented by 1200 lb. The first sizing condition is a maximum takeoff weight condition. The second is a 500 foot per minute cruise climb at 10,000 feet. The sizing mission is two separate flights of 37.5 nm. with a 10-knot headwind and 20-minute reserve. Table 1 shows a breakdown of one flight into segments including taxi, hover, transition, climb, cruise, and descend. The variables in the table denote parameters that will change based on the performance and capabilities of the different reference vehicles. These segments are visualized in a mission profile in Figure 6. More information about the analysis that was performed for determining this mission can be found in [4].

Six performance conditions measure the performance of the aircraft. The first three conditions find a best range cruise speed, best endurance cruise speed, and maximum cruise speed. Best range cruise speed is the speed at which the aircraft will travel the furthest, best endurance speed is the speed at which the aircraft will travel for the longest amount of time, and maximum speed is the absolute fastest the aircraft can fly in level flight. The next three conditions are speed sweeps at sea level, six thousand, and ten thousand feet elevation to look at the power requirements at different altitudes. For this design, the speed sweep range is 130 to 200 knots to capture the correct cruise speed range of the tiltrotor.

Initial Design Point

Disk Loading and Wing Loading

To reach an initial design point, sweeps are run in NDARC to determine how design parameters affect the sized aircraft. The baseline model is then adjusted towards an initial design point for the mission. Design parameters to sweep include rotor disk loading, wing loading, blade number, and rotor tip speed. Dependent parameters to minimize include design gross weight, fuel consumption, power, and cost.

Disk loading is a ratio in pounds per square foot (psf) of the aircraft thrust (gross weight when in hover) and the rotor disk area. Tiltrotors typically have a higher disk loading than helicopters, but less than tiltwings, lift fans, and jets [17]. Disk loading sweeps were performed on the initial models; results are shown in Figure 7-8.

Table 1. Sizing mission segments

Segment	1	2	3	4	5	6	7	8	9	10
Segment Type	Taxi	Hover	Transition	Climb	Cruise	Transition	Hover	Descend	Taxi	Reserve
Initial Alt. (MSL ISA)	6,000	6,000	6,050	6,050	10,000	6,050	6,050	6,050	6,000	10,000
Final Alt. (MSL ISA)	6,000	6,050	6,050	10,000	10,000	6,050	6,050	6,000	6,000	10,000
Time (sec)	15	30	10	t_{climb}	t_{cruise}	10	30	30	15	1,200
Distance (nm)	-	0	0	D_{climb}	37.5-D_{climb}	0	0	0	0	-
Speed	-	-	0	V_y	V_{br}	0	0	-	-	V_{br}
ROC (ft/min)	-	100	0	≥ 900	0	0	0	-100	-	0
Percent of Max Power	10	100	100	P_{climb}	P_{cruise}	100	100	100	10	P_{cruise}

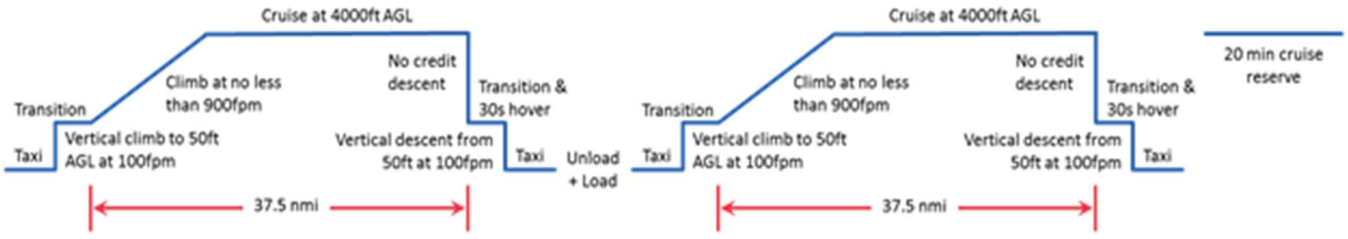

Figure 6. Sizing mission profile

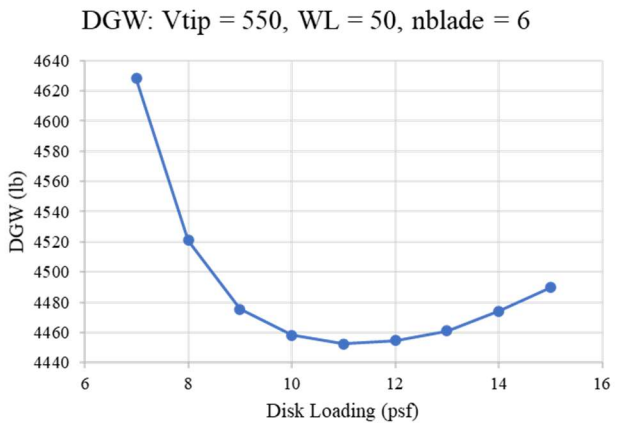

Figure 7. Turboshaft initial disk loading sweep

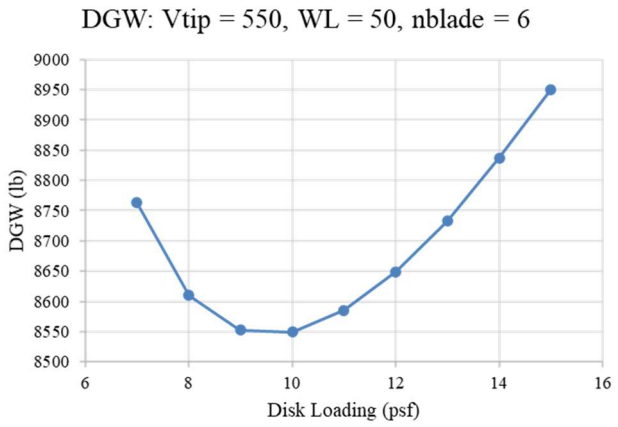

Figure 8. Electric initial disk loading sweep

The turboshaft has a clear DGW minimum at 11 psf so that point is chosen, but the electric has two very similar values for 9 and 10 psf. To choose between the points, the power was considered for the electric variant (Figure 9). A disk loading of 9 psf requires less power so it was chosen as the design point.

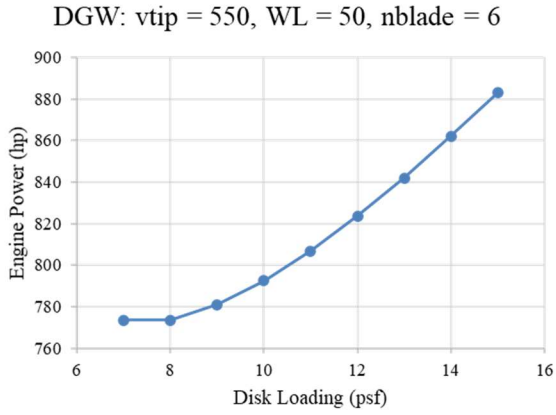

Figure 9. Electric power required

Now, fixing the disk loading to 11 and 9 psf for the vehicles respectively, a wing loading sweep is performed in Figure 10-11.

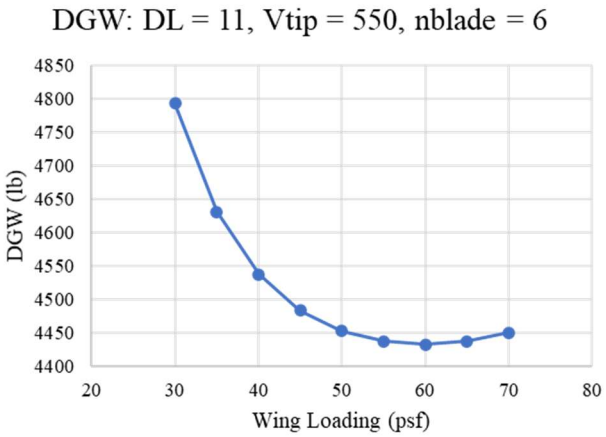

Figure 10. Turboshaft wing loading sweep

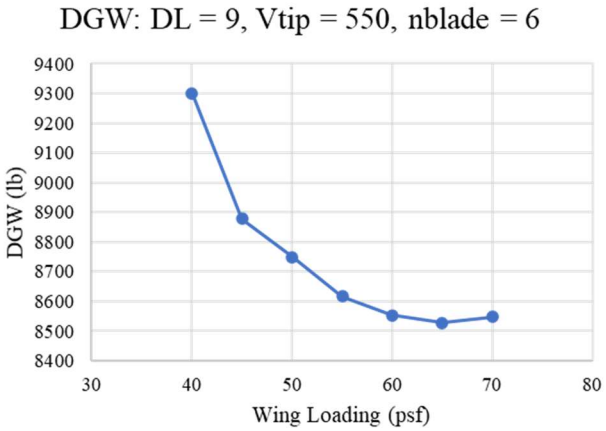

Figure 11. Electric wing loading sweep

Both models benefit from increased wing loading, with the electric model receiving a weight reduction of about 200 lb. The new wing loadings are 60 and 65 psf for the turboshaft and electric respectively. This now warrants another disk loading sweep, shown in Figure 12-13.

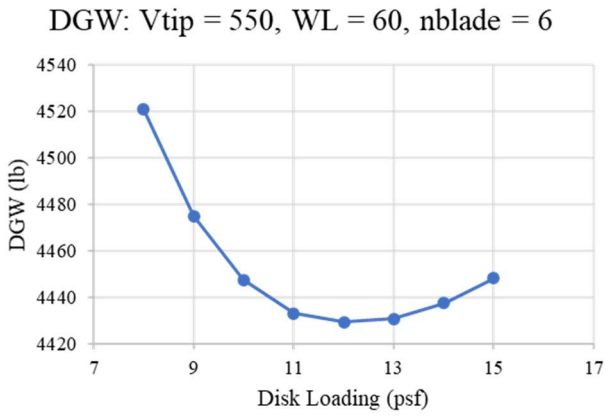

Figure 12. Turboshaft second iteration disk loading sweep

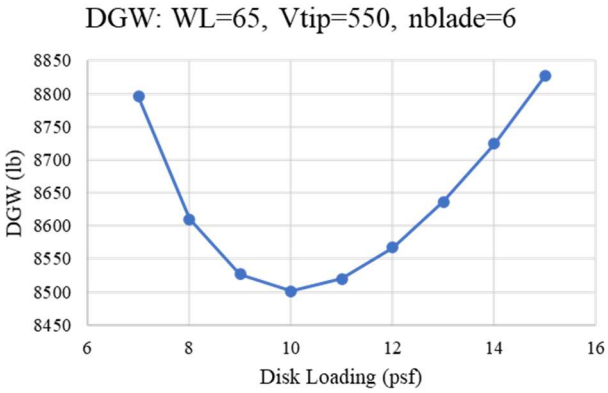

Figure 13. Electric second iteration disk loading sweep

The new design point for the turboshaft is a disk loading of 12 and a wing loading of 60 psf, and for the electric a disk loading of 10 and wing loading of 65 psf.

Hover Tip Speed

The NASA reference vehicles all are designed with a hover tip speed of 550 ft/s. This may not be the optimal tip speed for the vehicles, but it was chosen to reduce noise for the UAM mission. The same approach was taken with the tiltrotor design. A tip speed sweep was performed to find the optimum point and determine the weight penalty for lowering to 550 ft/s. The turboshaft sweep is shown in Figure 14. The optimal speed is 650 ft/s, but 550 ft/s adds only about 30 lb to the DGW, which is an acceptable tradeoff for the expected noise benefits.

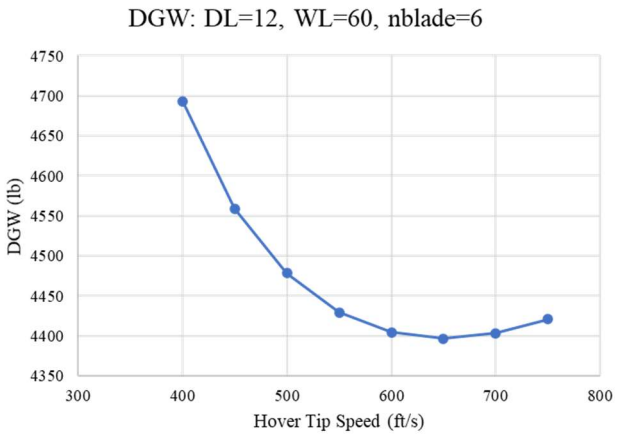

Figure 14. Turboshaft hover tip speed sweep

The electric variant has an optimum tip speed at about 700 ft/s and faces about a 150 lb weight penalty to use 550 ft/s, but 550 ft/s is again used for consistency with the other vehicles and noise considerations.

Number of Blades

The number of blades was chosen to accommodate the optimal disk loading of the aircraft, while considering engineering limitations of the rotor hub. A gimballed hub faces kinematic restrictions (due to requirement for pitch-flap coupling) when using more than 3 blades. This tiltrotor design uses a hingeless hub that allows for more rotor blades. If a blade number sweep is performed in NDARC, it will output that more blades will always produce a lighter aircraft, because the control weight is based on rotor chord. However, NDARC does not take into consideration the physical limitations of a hub, or material properties of the blade. Thus, blade number was based on blade aspect ratio, and an aspect ratio of close to 10 was chosen to match the XV-15's blade aspect ratio. 6 blades puts both variations in the correct aspect ratio region, and is physically possible to fabricate with a hingeless hub.

CAMRADII Rotor Performance Model

NDARC implements a low-fidelity rotor model in its analysis. CAMRADII [18] is a mid-fidelity comprehensive analysis tool that can be used to improve the rotor model used in the NDARC model. The rotor is modeled as a single, isolated rotor in a wind tunnel in both hover and cruise configurations. Operating conditions from NDARC are implemented into the hover and cruise wind tunnel configurations to optimize the rotors for the mission conditions.

CAMRADII rotor models use 2D airfoil tables for analysis, as the airfoil section has a significant impact on the performance. For this model, airfoil tables from NASA's Large Civil Tiltrotor (LCTR) [19] are used. Designing an airfoil deck is an extensive process and outside of the scope of this research, using airfoils designed for another tiltrotor

provides more accuracy than a standard airfoil deck such as the NACA 0012.

With the airfoil chosen, the parameters that are optimized with this analysis are twist and taper. For this study, linear twist and taper will be analyzed. Most tiltrotors that slow the rotor by 50% from hover to cruise have an ideal twist around -30 degrees, so a twist sweep from -20 to -40 degrees is expected capture the optimal point. The twist sweep is run for taper ratios at .425 (HECTR taper), then 0.5 to 1.0 (no taper) in increments of 0.1. To ensure consistency between blades of different chord distributions, the thrust-weighted chord (chord at 75% of the radius) is kept constant for all taper ratios. Varying with chord are two parameters that are stall delay factors, affecting the stall characteristics along the radius of the blade. They are calculated separately in a spreadsheet and varied as part of the input along with chord.

Rotor Model

Rotor radius, blade number, solidity, tip speed, and mass properties are taken from the NDARC model. Pitch link placement is informed by a previous tiltrotor CAMRADII model. This rotor will be modeled as a rigid rotor with free wake.

Hover Condition

Takeoff atmospheric conditions, C_T/σ, and tip speed were taken from the NDARC model for the twist and taper sweep in hover. Figure of merit is a measure of hover efficiency, and is calculated as $FOM = W(W/2\rho A_{ref})^{1/2}/P$, where W is weight, ρ is air density, A_{ref} is rotor disk area, and P is power. Figure 15-16 show the figure of merit for the turboshaft and electric variants. The turboshaft cases were run with taper ratios of 0.425 (HECTR) to 1.0, and twists from -10 to -40 degrees. The untapered blade has the highest figure of merit, and therefore the best hover performance. Note the electric variant twist and taper sweep was performed after the turboshaft, and the scope was narrowed based on the results from the turboshaft case to save computation time. The electric case uses taper from 0.8 to 1.0 and twist from -25 to -40.

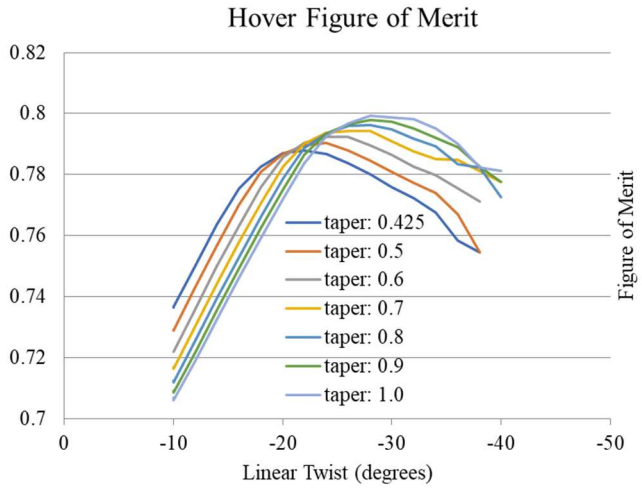

Figure 15. Turboshaft hover figure of merit

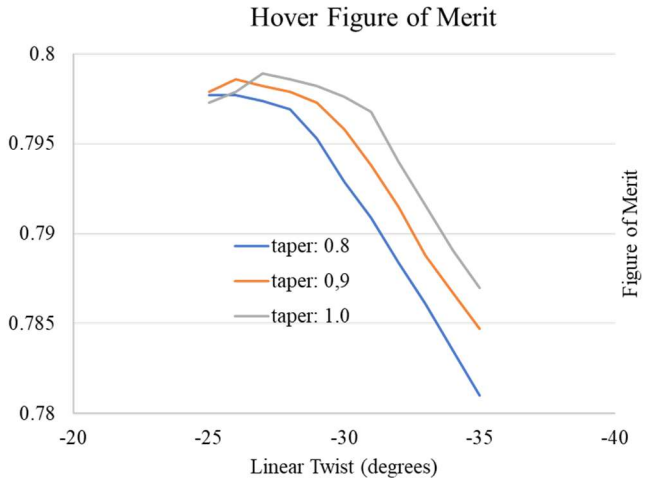

Figure 16. Electric hover figure of merit

Cruise Condition

Cruise atmospheric conditions, C_T/σ, flight speed, and tip speed were taken from the NDARC model for the twist and taper sweep in cruise. Propulsive efficiency (η), defined as parasite power (thrust, T, times velocity, V) over total power (η =), is the measure used for determining forward flight performance. Figure 17-18 show the propulsive efficiencies of all the twist and taper combinations in cruise. Note the same strategy as described in the hover case was implemented for the electric model again.

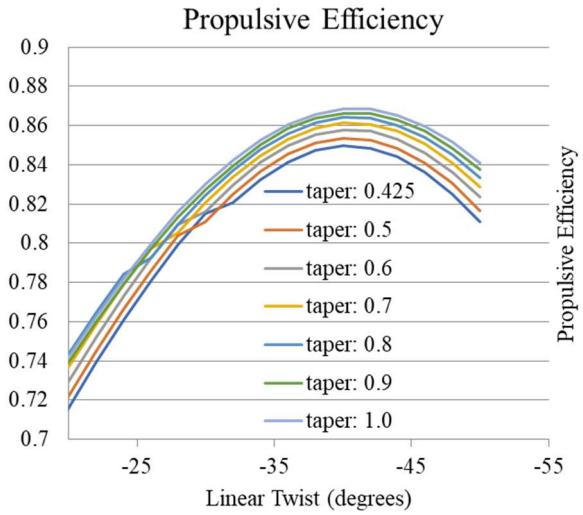

Figure 17. Turboshaft propulsive efficiency

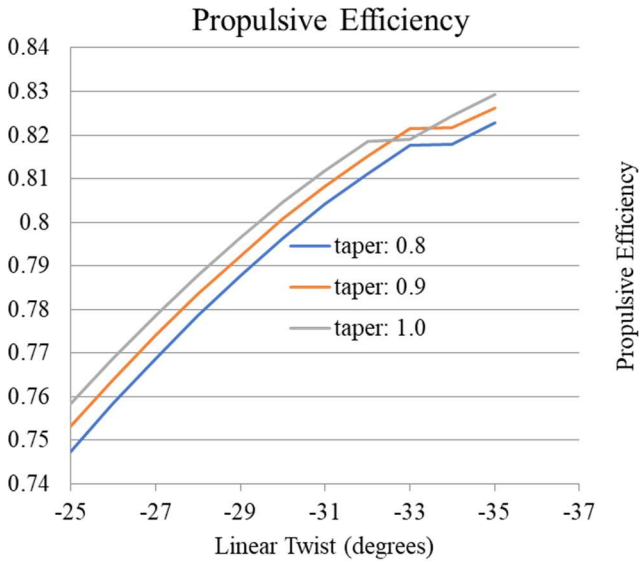

Figure 18. Electric propulsive efficiency

To find the best operating points for the aircraft, both hover figure of merit and propulsive efficiency need to be considered. Plotting hover figure of merit vs propulsive efficiency for each twist and taper combination produces a point distribution in which promising points can be chosen from the Pareto front to be put back into NDARC to resize the aircraft. The points chosen from the Pareto front include the point of highest hover figure of merit and point of highest cruise efficiency. Points in between are also examined, as the solution could fall between the two depending on the effects of hover and cruise performance on this mission. Figure 19-20 show the point distributions of the turboshaft and electric.

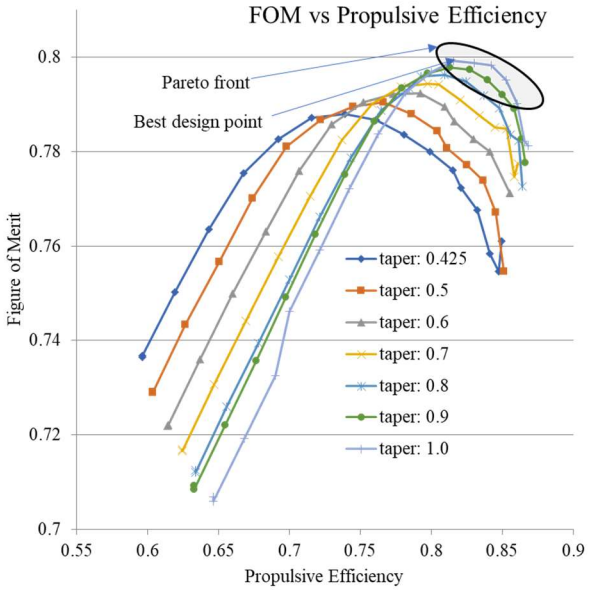

Figure 19. Turboshaft twist and taper design points

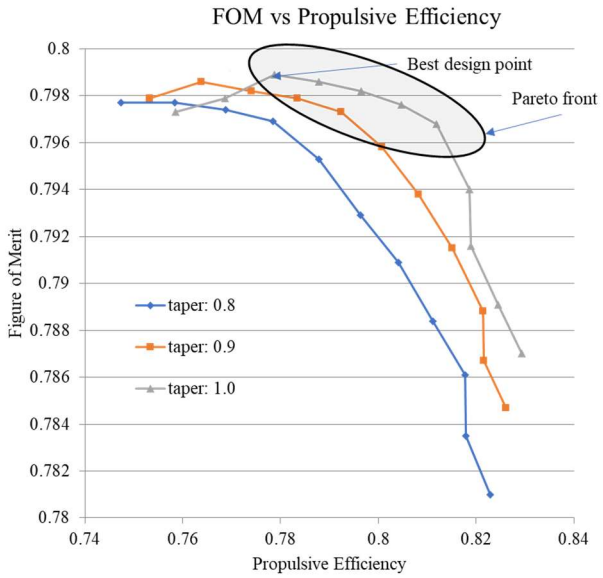

Figure 20. Electric twist and taper design points

In both cases, the points on the pareto front all have a taper of 1.0. To determine which twist and taper is best, the induced power coefficient and mean drag coefficient are taken from the rotor model of chosen points from the Pareto front. These parameters are put into NDARC, replacing the values from the original rotor performance model. The NDARC sizing is then run for each point to see the effect they have on sizing. In both cases, the optimized rotor significantly reduced the gross weight. The effects of the improved rotor model on gross weight are shown in Figure 21-22.

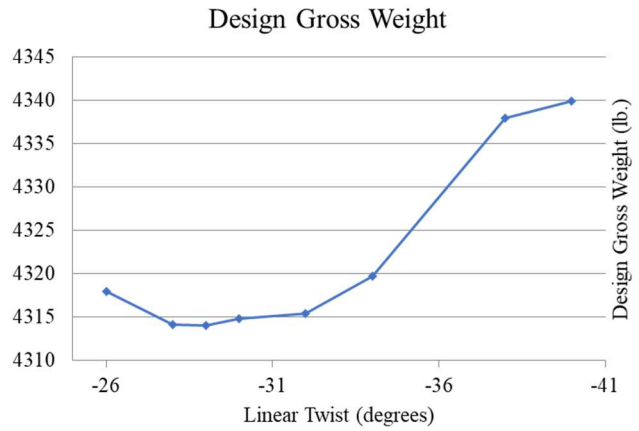

Figure 21. Turboshaft sizing at twist and taper design points

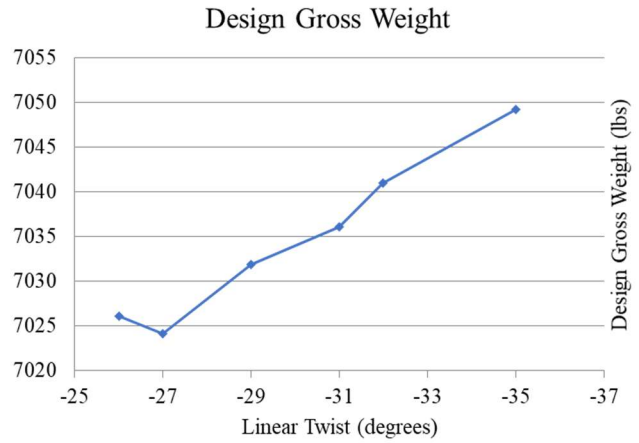

Figure 22. Electric sizing at twist and taper design points

For this design, the point that reduced the gross weight the most was chosen. The turboshaft operating point is a taper of 1.0 and a twist of -29 degrees, reducing the gross weight from 4429 lb to 4314 lb. The electric operating point is a taper of 1.0 and twist of -27 degrees, and reduced the gross weight by almost 1500 lb from 8501 lb to 7024 lb.

NDARC Rotor Model

Now that the rotor properties have been selected, the NDARC rotor model must be completely updated to reflect the performance of the CAMRADII rotor. NDARC uses polynomial equations to determine values for the induced power coefficient and the mean drag coefficient for different levels of thrust and advance ratios (cruise speeds). This design will focus on matching the conditions for hover and cruise.

To create these models, more data is needed from CAMRADII over a larger range of operating conditions. A collective sweep from 8 degrees to 23 degrees in hover conditions was performed to determine variations of induced power coefficient (kappa) and mean rotor drag coefficient (Cd mean) with changing thrust. The coefficients of the polynomial in the NDARC models are varied to accurately reflect hover conditions. Figure 23-26 show the NDARC polynomial models (dotted line) and the CAMRADII results in hover (solid line) for the two vehicles. The CAMRADII may vary slightly from the polynomial curve, but the accuracy is greatly increased from the original rotor model.

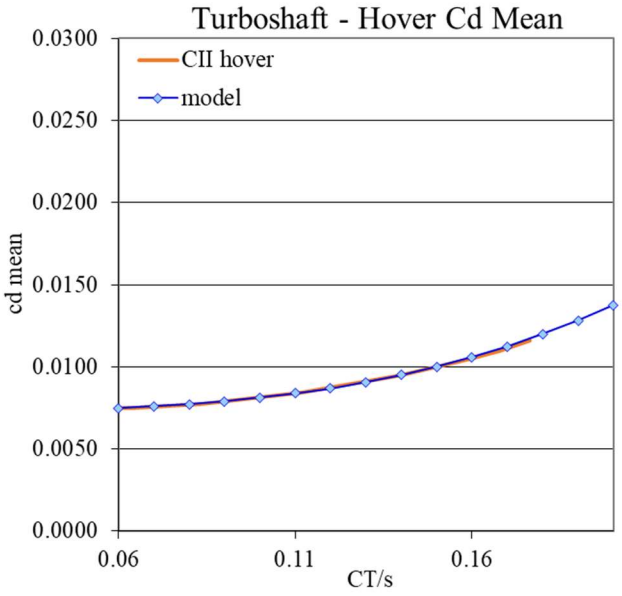

Figure 23. Turboshaft hover Cd mean model vs CAMRADII

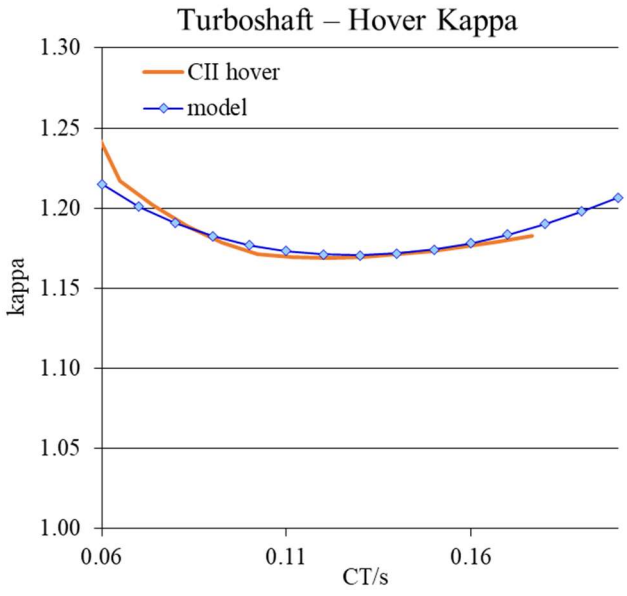

Figure 24. Turboshaft hover kappa model vs CAMRADII

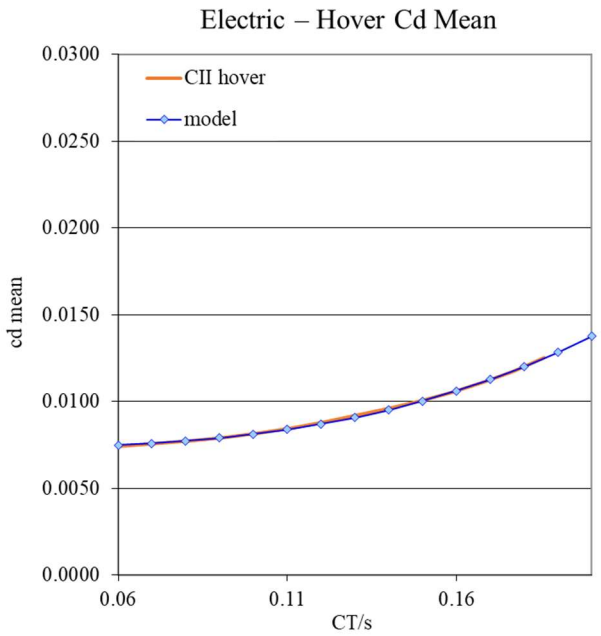

Figure 25. Electric hover Cd mean model vs CAMRADII

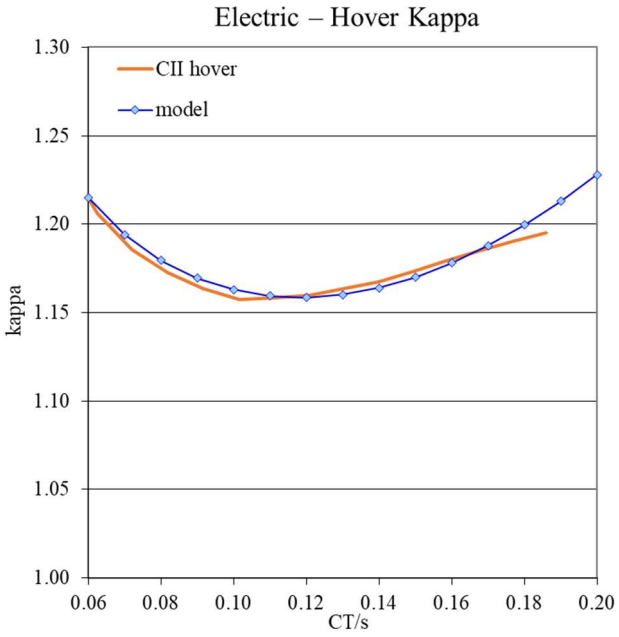

Figure 26. Electric hover kappa model vs CAMRADII

To calibrate the rotor model for forward flight, speed sweeps were run from 100 to 200 knots at different levels of thrust. Since thrust is equal to aircraft drag in steady, level flight, the thrust was controlled by trimming to 75%, 100%, and 125% of the NDARC aircraft drag value (D/q) in cruise. The results are plotted in terms of μ_z (muz), which is the ratio of forward flight speed to rotor tip speed. The plots for cruise for the two variants are shown in Figure 27-30.

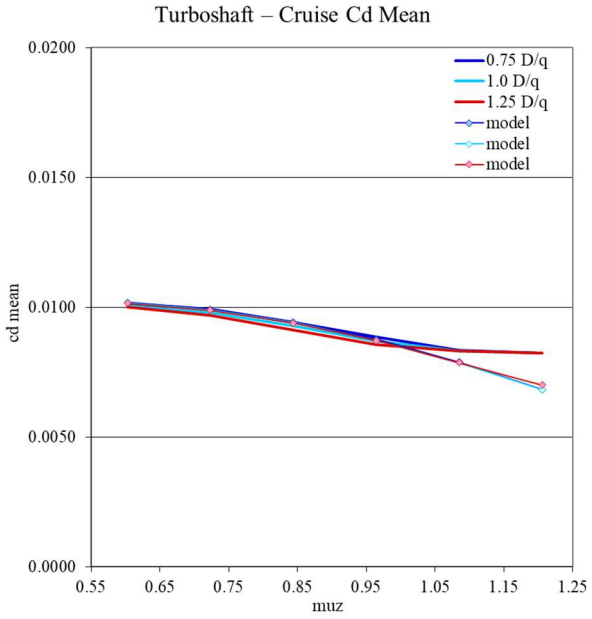

Figure 27. Turboshaft cruise Cd mean model vs CAMRADII

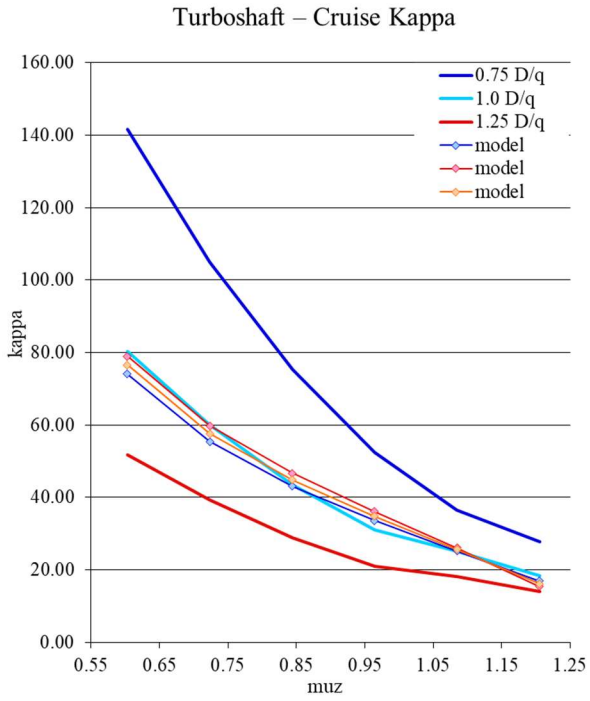

Figure 28. Turboshaft cruise kappa model vs CAMRADII

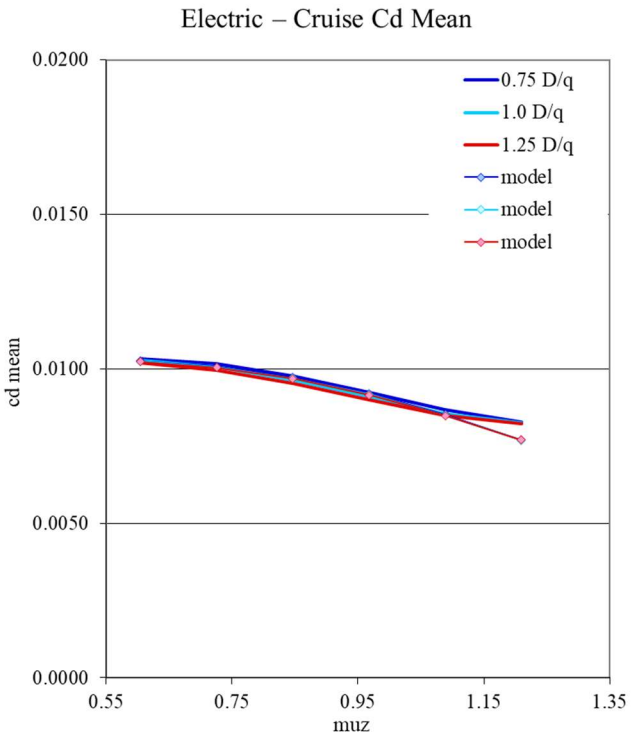

Figure 29. Electric cruise Cd mean model vs CAMRADII

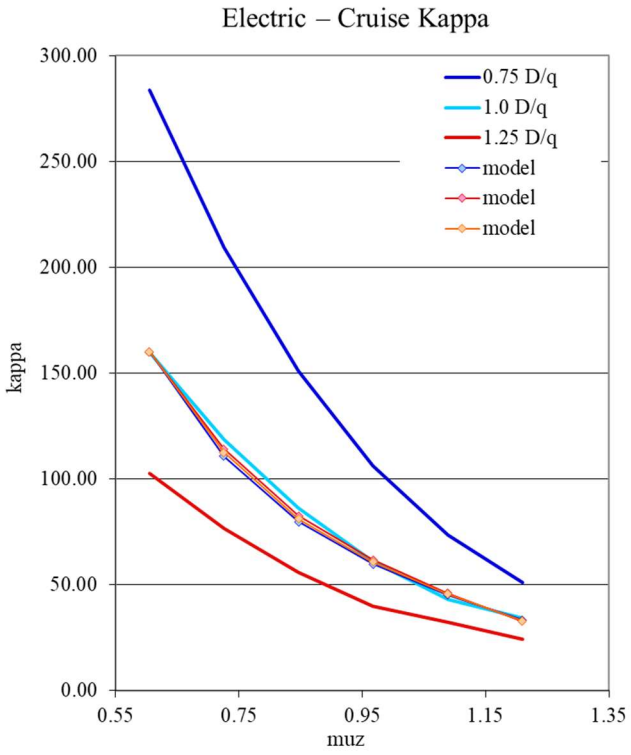

Figure 30. Electric cruise kappa model vs CAMRADII

The kappa plots in cruise show that NDARC is not currently able to model the large variation between induced power coefficients at different drag values for axial flight. Because of this, the drag value for the actual cruise mission condition was chosen to fit the model to, as that condition needs to be the most accurate. Most rotorcraft fly in edgewise forward flight, and that was the priority when this part of NDARC was designed, but tiltrotors in axial forward flight encounter greater kappa variations than would be seen in the edgewise forward flight of a typical rotorcraft. In this case it is outside of the bounds that the curve fit was designed to accommodate. One of the goals of the NASA reference vehicles is to find areas that the design tools can be improved. Here one has been found, and there will be an improved tiltrotor induced power model in a future NDARC version.

The rotor performance parameters are updated in the NDARC model based on the curves found in the rotor model spreadsheet, and the aircraft is resized. If the new aircraft is greatly different from the pre-CAMRADII model, the CAMRADII process may be run again with this new starting point. For the purposes of this research, only one iteration was performed. The new sized aircraft are the final NDARC models.

RESULTS

Aircraft Summary

The design process resulted in two NDARC aircraft models, one electric and one turboshaft tiltrotor. The vehicles are designed with the advanced technology of the High Efficiency Civil Tiltrotor [9], including composite structural construction and advanced drive system materials. They feature a two-speed transmission that reduces the rotor speed to about 50% in cruise, requiring a stiff, lightweight rotor to handle the speed variation. Through the process described in the previous section, the vehicles became more optimized to the UAM mission, creating lighter, better performing aircraft more representative of what is possible for tiltrotors in UAM. Figure 31-34 show CAD models of the final tiltrotor designs, created in SOLIDWORKS. More drawings can be found in the Appendix.

Figure 31. Turboshaft in hover

Figure 32. Turboshaft in cruise

Figure 33. Electric in hover

Figure 34. Electric in cruise

Dimensions

The NDARC output contains component dimensions for systems and subsystems of the sized aircraft. The majority of the dimensions are a result of sizing to the mission, with a few fixed values. The fuselage has set dimensions, but all other physical dimensions are sized for the mission. Table 2 shows key dimensions of the vehicles.

These dimensions are used to create the CAD models of the aircraft in Figure 31-34 and the Appendix in SOLIDWORKS [20]. At this conceptual design level, a generic fuselage shape is created, and generic wing and tail airfoils are selected based on thickness values. The CAD model allows for the visualization of relative sizes and spacing of the vehicle components and provides a visual representation of the different sizing requirements for turboshaft and electric aircraft.

Aiden Propulsion Topology

AIDEN [21] is a GUI for NDARC, and includes the ability to view the propulsion topology of NDARC models. Figure 35-36 show the propulsion topology for each aircraft. Each component type has a specific shape. Rotors are circles, propulsion groups are trapezoids, engine groups are hexagons, and fuel tanks are squares. Green items denote chemical components, blue items denote electric, and yellow denotes mechanical. Following the same coloring scheme, the shape outlines show how the component interfaces. Figure 35 is for the turboshaft. Fuel goes from the fuel tank component into each engine group (turboshaft engine). The engine groups convert the chemical energy to mechanical energy and send it to the propulsion group. The propulsion group is all the drive shafts and gear boxes between the engine and the rotor. The rotor gets mechanical energy from the propulsion group and the orange arrow denotes direction of spin for each rotor. Figure 36 is the electric variant. The topology is identical, except the fuel tank is replaced with a battery and the turboshaft engines are replaced with electric motors. In NDARC, batteries are modeled as fuel tanks that maintain constant weight through discharge and are adjusted to match energy density and discharge characteristics.

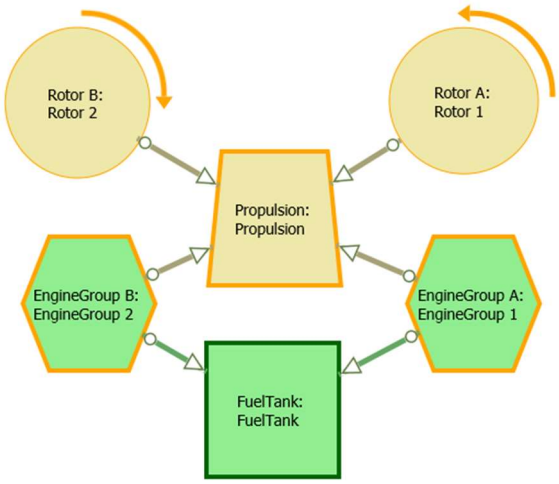

Figure 35. Turboshaft propulsion topology

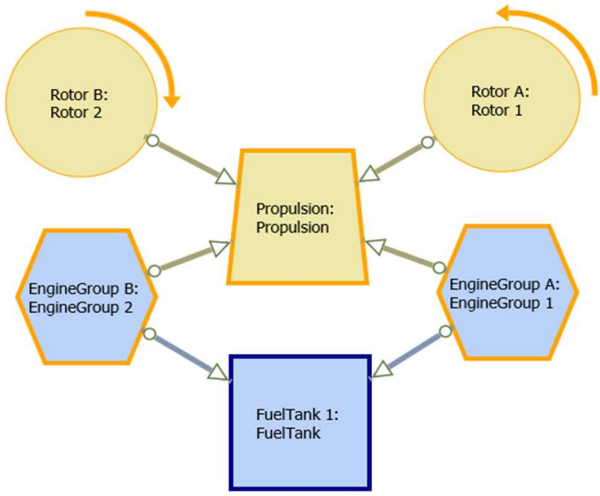

Figure 36. Electric propulsion topology

Table 2. Aircraft dimensions

UAM Vehicle	Turboshaft	Electric	UAM Vehicle	Turboshaft	Electric
Rotor			Tail		
Disk Loading (psf)	12	10	Area (sq. ft)	14.4	26.7
Number of Blades	6	6	Span (ft)	7.0	9.5
Radius (ft)	7.55	10.60	Chord (ft)	2.1	2.8
Chord (ft)	0.68	0.79	Dihedral Angle	34.2	35.0
Solidity	0.1713	0.1428	Fuselage		
Taper Ratio	1.0	1.0	Length(ft)	30	30
Aspect Ratio	11.1	13.4	Width(ft)	6	6
Lock Number	7.95	8.99	Height(ft)	5.1	5.1
Wing			Engine		
Wing Loading (psf)	60	65	MRP per Engine (hp)	411	638
Wingspan (ft)	24.0	30.5	MCP per Engine (hp)	323	425
Chord (ft)	3.0	3.6	Specific Fuel Consumption	0.56	-
Wing Area (sq. ft)	71.7	108.5	Weight/Power (lb/hp)	0.34	-
Aspect Ratio	8.1	8.5	Fuel Capacity (lb.)	195.8	-
Thickness	0.2	0.2	Battery Weight (lb.)	-	1,950
Sweep (degrees)	-3.76	-3.76	Energy Storage (MJ)	-	1,274
Dihedral (degrees)	4.65	4.65			

Weights

Weights are determined in NDARC using parametric equations built from weight models based on historical aircraft, with a technology factor to improve the weight based on current or expected future technology. Weight is determined on a component basis and summed to estimate the entire aircraft weight. In this model, passenger weight is fixed

at 1200 lb and weights such as cabin furnishing, environmental control and auto flight controls are fixed, resulting in 438 lb of fixed weight. All other weights in the model are sized using the parametric weight equations. Table 3 breaks down the weights by category for both variations. There is also a column showing the percent difference in weight between the two vehicles. The electric version is 64% heavier overall, and it's clear that the weight increase is driven by the battery weight. The battery of the electric is 1700 lb heavier than the fuel system (including fuel) of the turboshaft (fuel/battery system weight 1950 lb vs. 247 lb). This weight increase propagates through the rest of the design, and the empty weight ends up being doubled for the electric model.

For the sizing mission, power required and power available show what segments were the driving conditions behind the engine sizing. Figure 37 shows the mission power characteristics for each vehicle. The segments that size the engines/motors are where the power required meets power available. Ignoring the taxi segments (which are flown at a specified power level), it is apparent that the turboshaft is sized by the hover condition. At all hover segments, the power required is very close to the power available. The opposite is true for the electric model, as the 900 foot per minute climb segment drives the sizing. There is plenty of margin during the hover segments. Hover is a fundamental requirement, so altering the mission wouldn't benefit the turboshaft. However, since the climb segment sizes the electric, re-

Table 3. Partial weight statement and increase percentages

Component	Turboshaft (lb)	Electric (lb)	Percent Change
DESIGN GROSS WEIGHT	4299.7	7053.4	64%
Struct Design GW	4299.7	7053.4	64%
Weight Max Takeoff	4643.7	7617.7	64%
WEIGHT EMPTY	2893.1	5843.8	102%
STRUCTURE	1222.1	1761.1	44%
wing group	190.2	286.5	51%
rotor group	159.8	340.8	113%
empennage group	14.4	32.1	123%
fuselage group	425.7	600.6	41%
PROPULSION GROUP	678	2709	300%
fuel system (with fuel)/battery	246.5	1949.9	791%
drive system	268.2	438.4	63%
SYSTEMS AND EQUIP	790.5	964.6	22%
flight controls	279.5	388	39%
hydraulic group	103	156.9	52%
electrical group	79.2	85.1	7%
Fuel for DGW	195.9	0	-100%

Performance

Aircraft performance is measured both for the sizing mission, and the off-design mission. The sizing mission performance measures how well the aircraft flies the UAM mission. Two of the most important parameters are fuel/energy burn and block time, the overall mission time. Table 4 contains some parameters from the sizing mission, and the off-design performance parameters of the first three performance conditions: best range speed, best endurance speed, and maximum speed.

evaluating the mission and changing the climb rate to a less aggressive value would reduce the power required, thus reducing the battery size and the overall weight and cost of the aircraft.

The results of the off-design speed sweeps at sea level, six thousand, and ten thousand feet altitude are shown graphically below in Figure 41 for the turboshaft and Figure 42-45 for the electric.

Table 4. Sizing mission and off-design performance

Sizing Mission Performance	Turboshaft	Electric
Fuel Burn (lb)	141	-
Energy Burn (MJ)	2,738	947
Air Distance (nm)	79.6	79.5
Block Time (min.)	32.3	31.4
Block Speed (kts)	139.1	143.1
Fuel Flow (lb/hr)	261.6	-
Energy Flow (MJ/hr)	5,078	1,806
Specific Range (nm/lb)	0.53	-
Specific Range (nm/MJ)	0.03	0.08
Fuel Efficiency (ton-nm/lb)	0.32	-
Energy Efficiency(ton-nm/MJ)	0.02	0.05
Flyaway Cost ($)	3,529,000	5,133,000
Yearly Operating Cost ($)	2,930,683	3,535,276
Cost Per Trip ($)	341	399
Off-design Mission Performance		
Best Range Speed (kts)	170.0	166.59
Best Endurance Speed (kts)	129.4	119.08
Maximum Speed (kts)	203.6	212.54

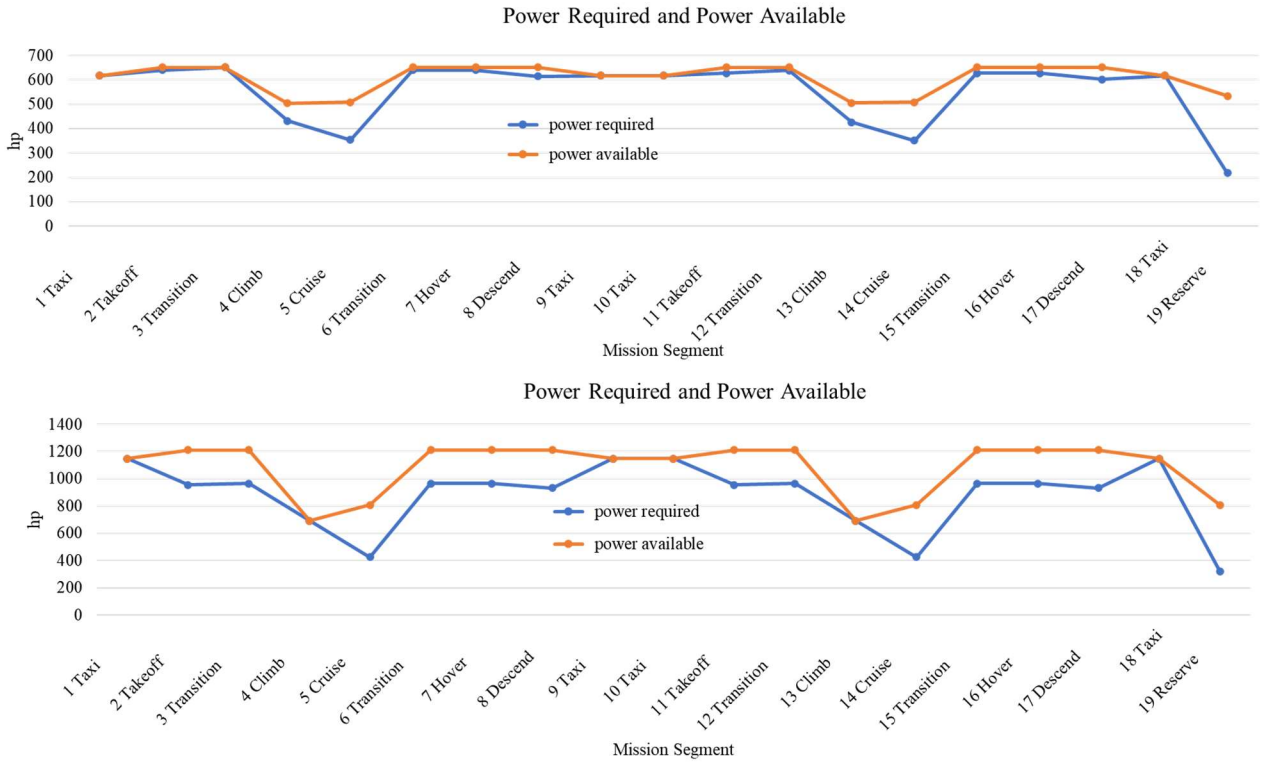

Figure 37. Mission power for turboshaft (top) and electric (bottom)

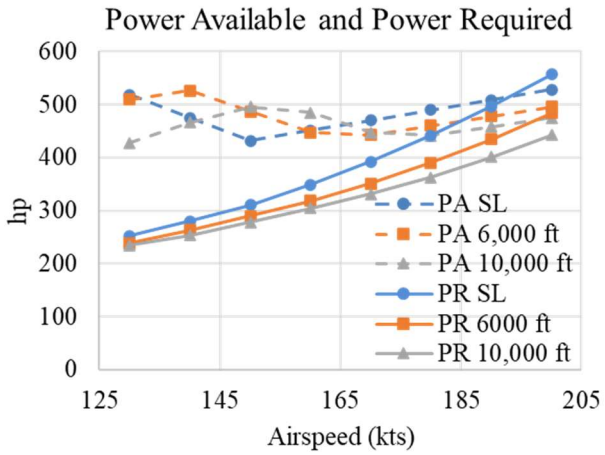

Figure 38. Turboshaft power available (PA) and power required (PR) - speed and altitude sweep

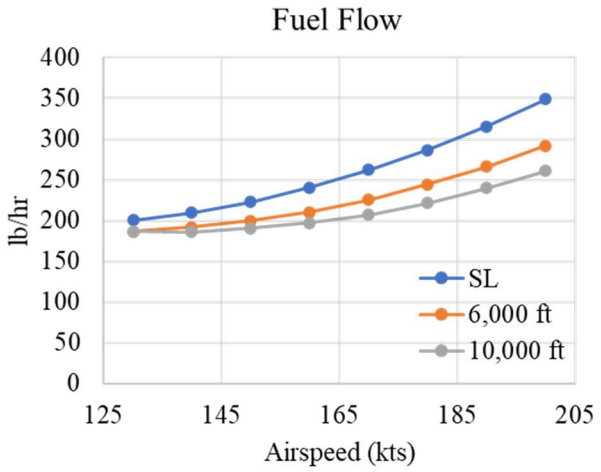

Figure 39. Turboshaft fuel flow - speed and altitude sweep

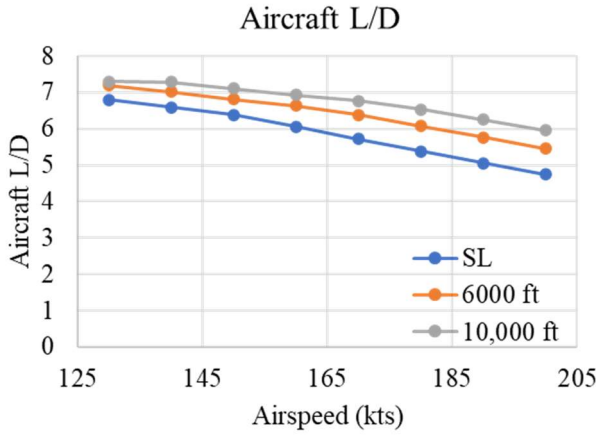

Figure 40. Turboshaft L/D=WV/P – speed and altitude sweep

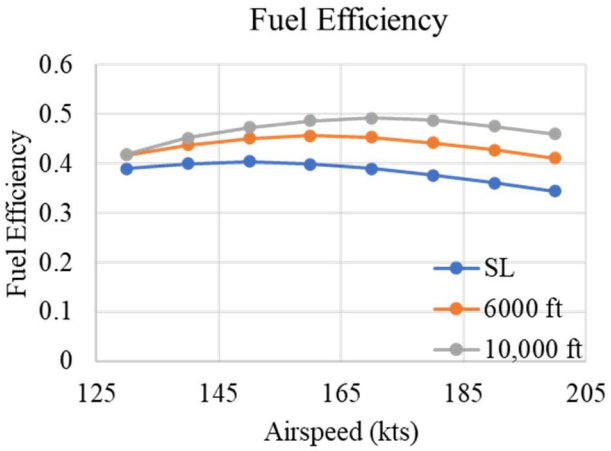

Figure 41. Turboshaft fuel efficiency - speed and altitude sweep

As the altitude increases, the margin between power available and power required increases because of reduced aircraft drag, increasing the maximum speed achievable. At sea level for the turboshaft, the power required exceeds the power available at 200 kts, meaning the top speed at sea level is between 190 and 200 kts. The previously mentioned maximum speed performance condition was calculated at 6,000 ft to be 203 kts, matching where the power required meets power available in this chart.

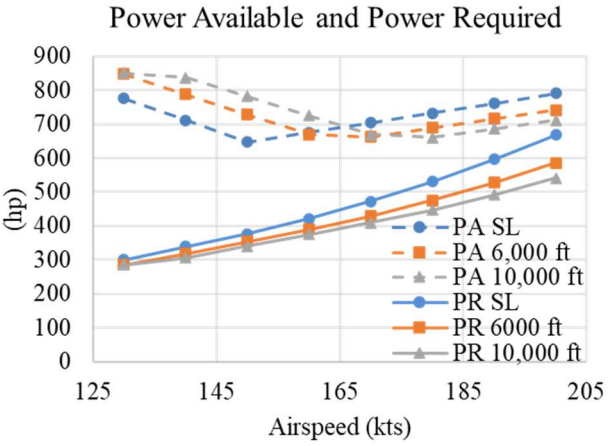

Figure 42. Electric power available (PA) and power required (PR) - speed and altitude sweep

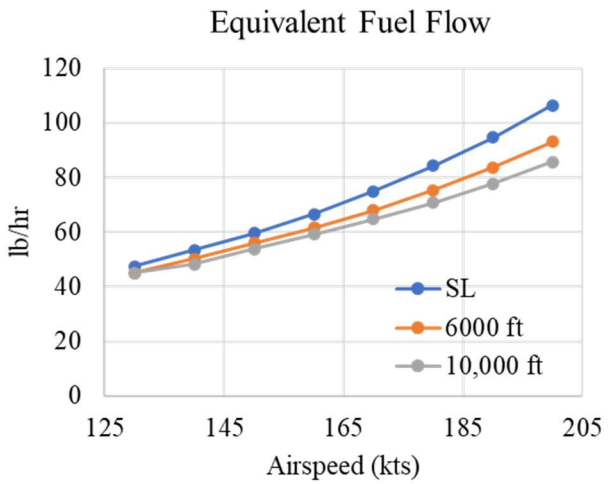

Figure 43. Electric equivalent fuel flow - speed and altitude sweep

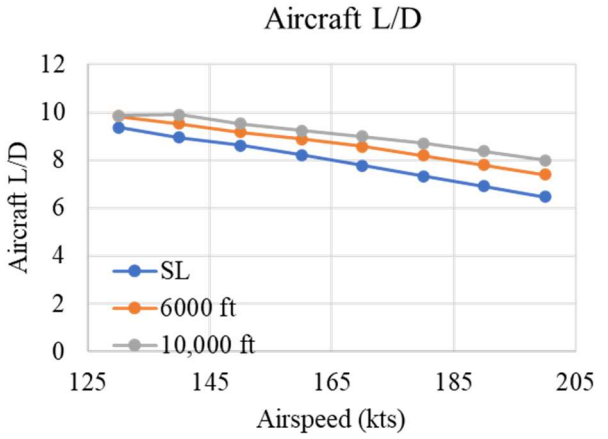

Figure 44. Electric L/D - speed and altitude sweep

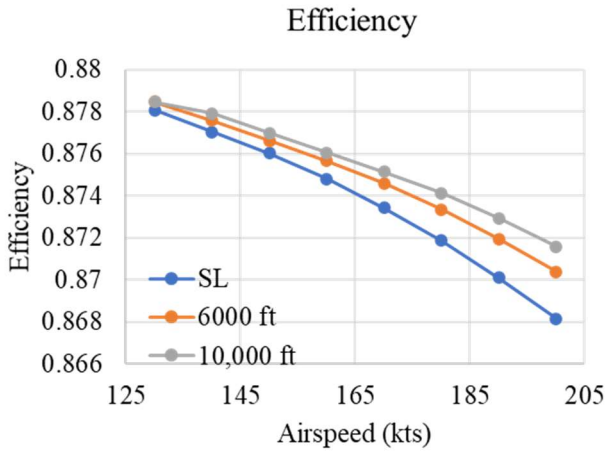

Figure 45. Electric efficiency - speed and altitude sweep

The fuel flow, aircraft L/D, and efficiency charts show that the aircraft gain efficiency with altitude. Above 10,000 ft is not considered because 10,000 ft is the maximum altitude for an unpressurized cabin, so that is the ceiling for the NASA UAM vehicles. Including a pressurized cabin increases weight, complexity, and cost that is not worth the tradeoff for the short range UAM flights. It does confirm that the cruise segment is ideally placed at the maximum altitude of 10,000 ft.

DISCUSSION

Comparison with Reference Vehicles

The other NASA reference vehicles were designed to the same mission for simple, direct comparison. Comparing the characteristics of these vehicles helps give insight into what configurations and design choices may be best suited for UAM application. Figure 47-50 show the comparison of turboshaft (blue) and battery electric (orange) parameters for weight, fuel/battery weight, power, and operating area of the tiltrotor, side-by-side, quadrotor, and lift+cruise. The legend for the following bar charts (Figure 47-56,58) is shown in Figure 46. Note, again, for the lift+cruise, the turboshaft version is turboelectric. In all charts presented in this section, the tiltrotor is in the first set of columns, followed by the side-by-side, quadrotor, and lift+cruise.

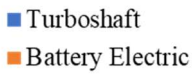

Figure 46. Bar chart legend

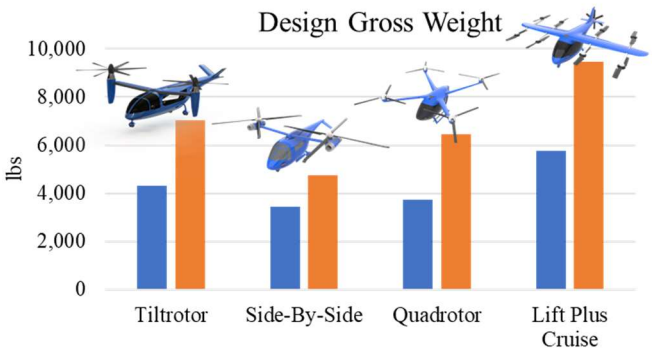

Figure 47. Reference vehicle design gross weight comparison

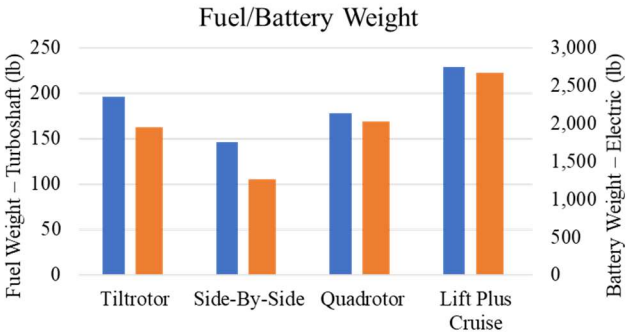

Figure 48. Reference vehicle fuel (left axis) and battery weight (right axis) comparison

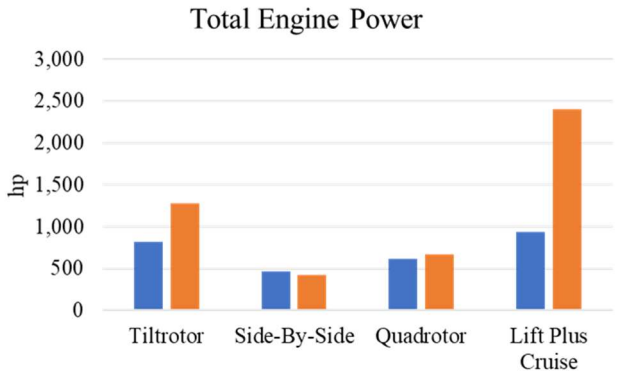

Figure 49. Reference vehicle total engine power comparison

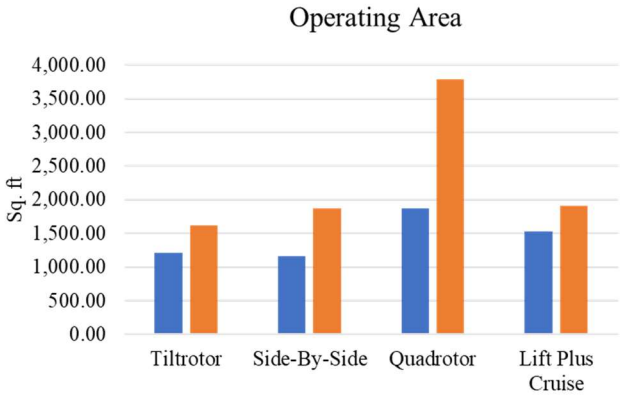

Figure 50. Reference vehicle operating area comparison

Emerging as the lightest aircraft is the side-by-side, followed by the quadrotor, tiltrotor and lift+cruise. This holds true for both turboshaft and electric varieties. The lift+cruise is significantly heavier than the rest of the configurations. Using one propulsion method for hover and another for forward flight means there will always be one propulsion method that is added dead weight at a given time, as well as adding the drag from the stopped rotors in forward flight.

The fuel weight follows the same relative pattern as design gross weight. The tiltrotor carries about 50 more lb of fuel than the side-by-side for the mission, or about 8 gallons. For the electric model, the tiltrotor manages to size a smaller battery than the quadrotor.

The tiltrotor has significantly greater installed power than the side-by-side and quadrotor, due to the higher disk loading (but also enabling higher maximum speed). The electric lift+cruise has extremely high power required, which correlates with its high disk loading as well.

Operating area is a metric of the aircraft's footprint, calculated from the length and the widest point, including the rotor blades. The tiltrotor has the smallest operational footprint of all the vehicles, which will be an important consideration for UAM as vertiports are integrated into urban areas. The less space the aircraft needs, the more areas become available for vertiports, and smaller vertiports will be cheaper to build.

Performance is where the added weight of the tiltrotor pays off. Increased cruise speed is the primary motivation for a tiltrotor, and Figure 51-53 show how this configuration increases the speed on all fronts.

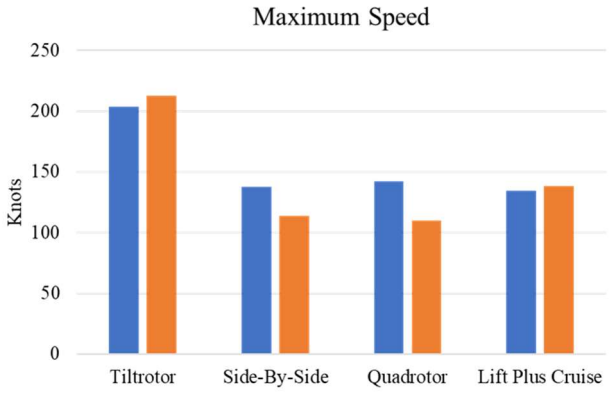

Figure 51. Reference vehicle maximum speed comparison

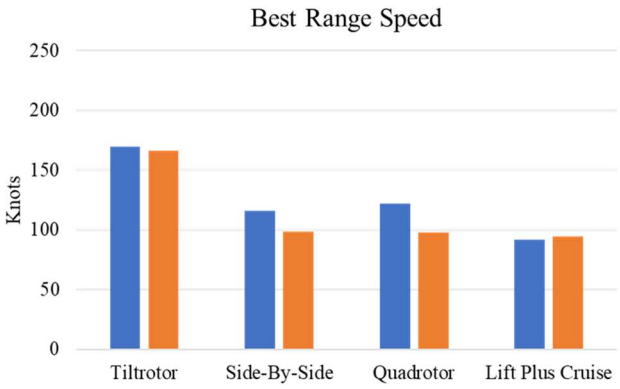

Figure 52. Reference vehicle best range speed comparison

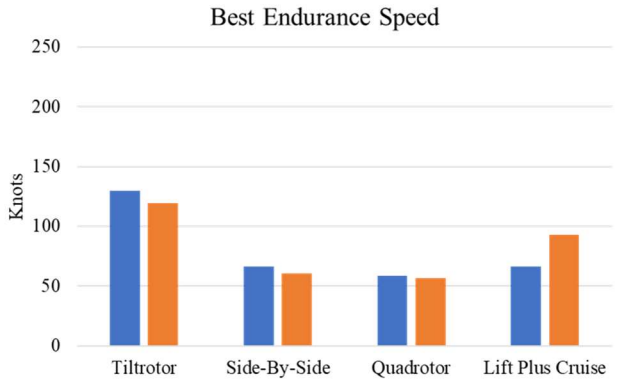

Figure 53. Reference vehicle best endurance speed comparison

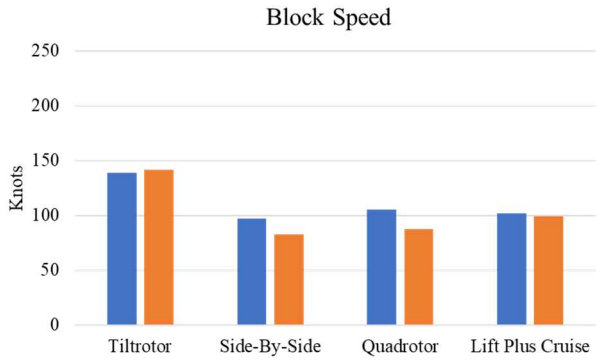

Figure 54. Reference vehicle block speed comparison

Maximum speed is not used in the mission for efficiency, but it is an important metric for understanding the capabilities of a vehicle. Maximum speed, as well as the other speed variations are notably higher for the tiltrotor in comparison to the other vehicles. The others are, for the most part, very similar in terms of speed (all under 150 kts), while the tiltrotor's maximum speed is over 200 kts for both variations. The electric tiltrotor at 212 kts top speed is almost twice as fast as the electric quadrotor at 110 kts. The more important metric for UAM application is block speed. Block speed is the average speed that the mission is conducted at, and it factors in all parts of the mission including hover and descent. While the other vehicles are between 80 kts and just over 100 kts, the tiltrotor averages about 140 kts for the entire mission, higher than most of the other vehicles' top speed. This speed results in a shorter time for the overall mission, shown as block time in Figure 55.

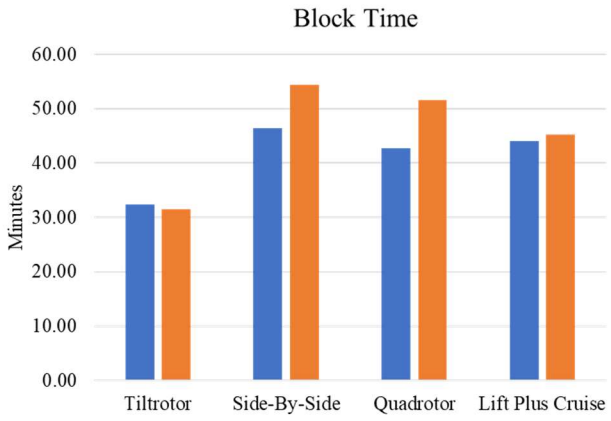

Figure 55. Reference block time comparison

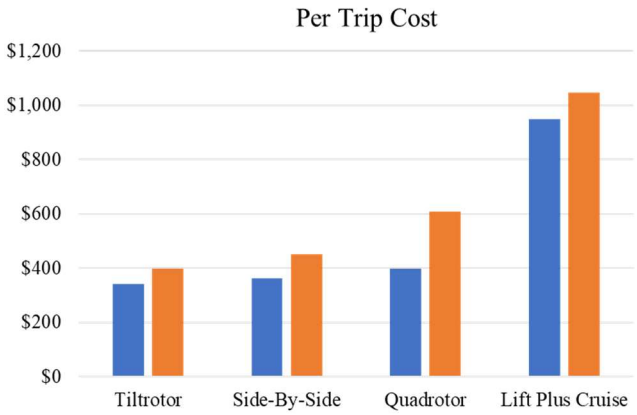

Figure 56. Reference vehicle per trip cost comparison

The tiltrotor comes in at just over 30 minutes of block time. 30 minutes to take off, fly 37.5 nm, land, take off again, and fly another 37.5 nm and land. This does not account for any loading or unloading time. The other vehicles are all right around 45 minutes, with the electric side-by-side at about 55 minutes. The side-by-side is the lightest vehicle and consumes the least fuel, but there is a tradeoff that it is also the slowest. Though the lift+cruise has a wing for improved efficiency in forward flight, it does not end up seeing any significant improvements in speed, likely due to increased drag from the stopped lifting rotors.

NDARC predicts costs based on the Harris-Scully cost model. Developed for shaft driven helicopters and turboprop aircraft, the model predicts aircraft purchase price, maintenance cost, and direct operating cost based on the statistical relationships of mostly civil aircraft. The model does account for electric component costs, but since the electric aircraft industry is not established, it is better to take the cost predictions as a relative measure to compare designs rather than an absolute cost.

The quick trip time translates into operational cost savings for the tiltrotor, shown in Figure 56. Per trip, it is the cheapest aircraft to fly. Though it consumes the second most fuel, it makes up for it with reducing the other costs associated with the trip, primarily maintenance. Less operating time results in cheaper flights. The standard NDARC cost model normally includes a crew cost, but since these vehicles are designed with autonomous operation the crew cost has been factored out of operation. Figure 57 presents a breakdown of the cost per trip into components of fuel, depreciation, insurance, finance, emission trading scheme (ETS), and maintenance.

Maintenance is the most influential component, then fuel consumption. The fuel cost for the electric vehicles is the cost of electricity to charge the battery. Maintenance is determined on a per flight hour basis, so flying the missions faster will require less maintenance per mission. The 9 rotors on the lift+cruise appear to cause increased maintenance costs in the model, and the high overall cost increases the depreciation factor as well. Though it is the largest factor, maintenance is also likely the most uncertain of costs. Since there is little data on electric aircraft, the cost model may not accurately reflect the maintenance cost of such aircraft. Developers of electric aircraft speculate the maintenance costs will be lower than previous aircraft due to the simplicity and reduced moving parts of electric motors [22].

Though the cost per trip is lower, the tiltrotor does come with an increased upfront cost for the aircraft, at least compared to the side-by-side and quadrotor. The aircraft costs are shown in Figure 58.

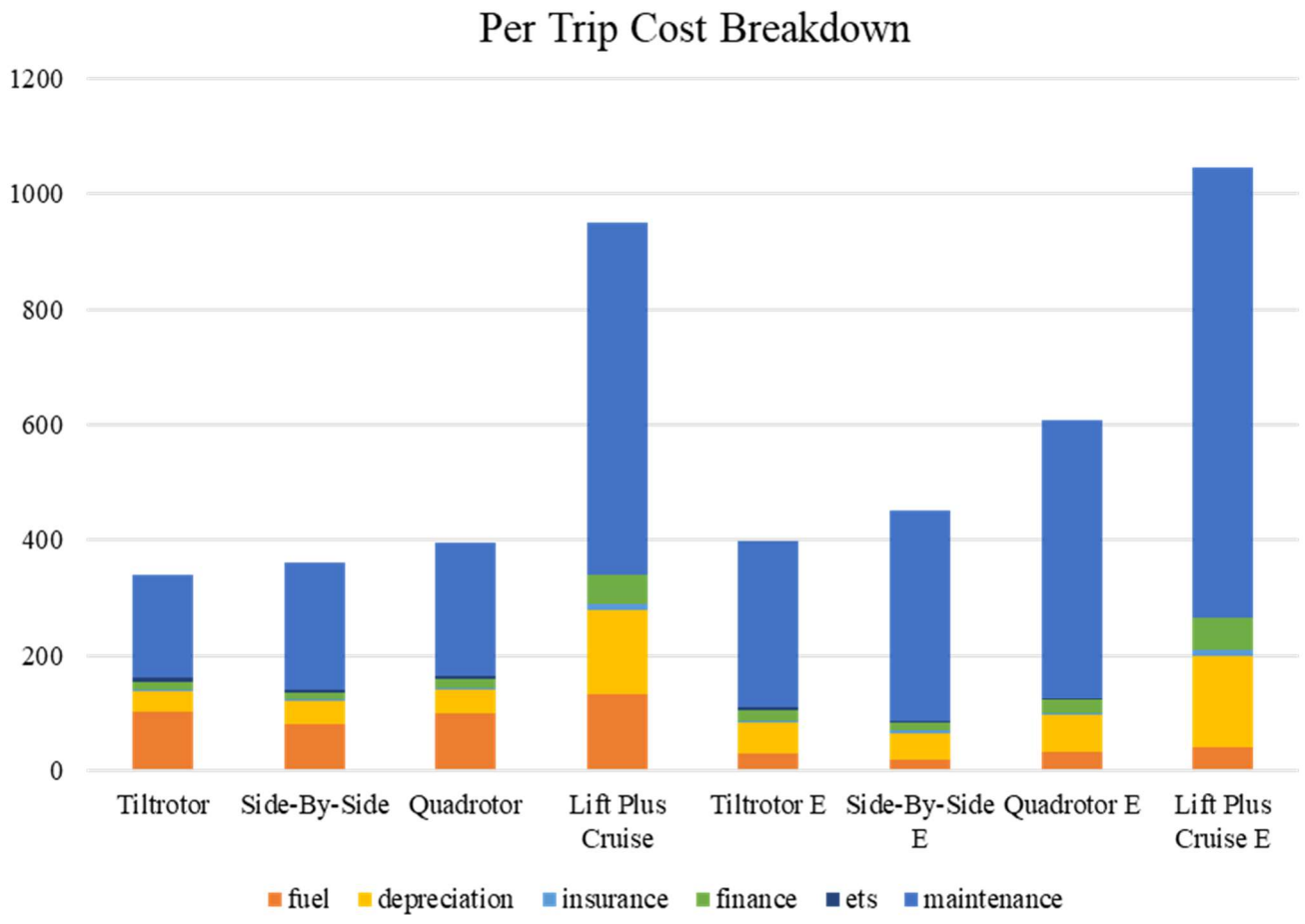

Figure 57. Reference vehicle breakdown of per trip costs

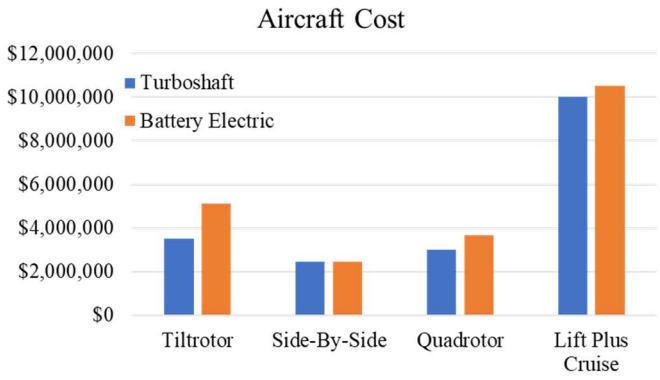

Figure 58. Reference vehicle cost comparison

Turboshaft to Electric Conversion

A core goal of UAM is to have all-electric aircraft for operation in cities for emissions as well as noise considerations, but it's important to compare the electric designs with conventional turboshaft counterparts. Unless battery energy density reaches several times the state of the art, battery electric aircraft large enough to carry passengers will nearly always be heavier than their turboshaft counterparts. The notable exception is if the configuration is not feasible to power with a turboshaft, namely, distributed electric propulsion with many rotors.

The multiple configurations were created in part to assess how characteristics of each type affected the performance for the UAM mission to assist industry in their designs. Each configuration was created with a turboshaft and battery-electric variant, except for the lift+cruise, where geometric constraints with the distributed propulsion system makes a pure turboshaft impractical, so a hybrid turboelectric and battery electric are used. The turboshaft model serves as a baseline for the overall configuration, and how the characteristics of the configuration affect the performance in the specified mission. An important question that these vehicles help answer is how will changing a vehicle to electric change its characteristics. Unfortunately, there do not appear to be concrete rules for how electrification will affect sizing and performance.

For all configurations, design gross weight increased for the electric version, but the amount of weight gain varied by design. The side-by-side only increased in weight by 38%, but the tiltrotor and lift + cruise increased by 64% and the quadrotor increased by the most with a 73% weight increase. Interestingly, the two winged vehicles both increased by the same percentage. That is not enough to determine causation, so more winged reference vehicles should be designed, such as a tiltwing or tiltrotor with many rotors, to see if the trend stands.

Installed power change varied greatly by configuration. The lift+cruise had the largest power increase at 79%, this is in part due to the fixed rotor radius of the lifting rotors. The aircraft became heavier, but the lifting rotors could not geometrically get any larger, so the disk loading was increased by 64%. This higher disk loading influenced the increase in power. The tiltrotor increased in power by 55% from turboshaft to electric, and the quadrotor increased by 10%. The side-by-side actually decreased in power by 9%, this is likely because the electric version optimized to a 30% lower disk loading value, so it is the opposite situation of the lift+cruise. The tiltrotor and quadrotor only reduced their disk loading by 17% and 14% respectively.

One parameter that did show consistency between models is rotor radius. The tiltrotor, side-by-side, and quadrotor all increased in rotor radius by about 40%. Lift+cruise had a fixed radius, so no scaling occurred. Rotor chord, aspect ratio, and solidity all changed by varying amounts, but all rotors ended up getting 40% larger in radius.

Electrification increases the aircraft cost of the tiltrotor the most, with a 45% increase. The side-by-side and lift+cruise cost increased less than 5% and the quadrotor only increased by 22%. Contrasting this is the per trip cost, where the tiltrotor and lift+cruise have the lowest increase at 17% and 10%, and the quadrotor tops the scales at 53% per trip cost increase.

For the side-by-side and quadrotor, speed attributes decrease about 15-20%. For the tiltrotor and lift+cruise the speeds are mostly within 3% of change with the electric versions actually being faster for some metrics. This causes the block time for the side-by-side and quadrotor to increase by about 20% while the tiltrotor and lift+cruise are within 3%.

Table 5 summarizes these variations, with colors indicating an increase or decrease from the turboshaft. The darker green indicates greater increase in that parameter and darker red indicates greater decrease.

Table 5. Percent change of parameters from turboshaft to electric

UAM Vehicle	Tiltrotor	Side-By-Side	Quadrotor	Lift Plus Cruise
Diskloading	-17%	-30%	-14%	64%
Rotor radius	40%	40%	42%	0%
Rotor chord	17%	-2%	22%	64%
Rotor aspect ratio	20%	43%	17%	-39%
Solidity	-17%	-30%	-14%	64%
Design gross weight	64%	38%	73%	64%
Empty Weight	102%	70%	124%	91%
Lock number	13%	25%	26%	0%
Power	55%	-9%	10%	79%
Aircraft cost	45%	0%	22%	5%
Cost per trip	17%	26%	51%	12%
Best range speed	-2%	-15%	-19%	3%
Best endurance speed	-8%	-9%	-3%	40%
Max speed	4%	-17%	-23%	3%
Block speed	2%	-15%	-17%	-3%
Cruise speed	-3%	-15%	-17%	-3%
Block time	-2%	17%	20%	3%

500 Nautical Mile Excursion

The UAM reference vehicles were all designed to fly 75 nm, and the tiltrotor shows speed improvements that translate to faster mission times for this mission. However, the benefits of a tiltrotor become even more apparent as the range increases. To better take advantage of the capabilities of a tiltrotor, an excursion of increasing the sizing mission range to 500 nm with the same 6 occupant payload was investigated. A new tiltrotor was sized to fly this longer mission, and then its performance on the standard 75 nm mission was compared to the tiltrotors described previously.

Sizing the tiltrotor to 500 nm greatly increases the variety of missions one vehicle can accomplish, and therefore the versatility and usefulness of the vehicle. The one vehicle could fly the UAM mission, and then fly an AAM mission to a remote area 250 miles away, and anything in between. One caveat here is that the vehicle sized for 500 miles can currently only be a turboshaft. An electric tiltrotor does not converge with the 500 nm mission, as the battery size required becomes too heavy.

The 500 nm tiltrotor was sized using the same process described throughout this paper and resulted in an aircraft in between the 75 nm turboshaft and electric variations. Figure 59-63 show the empty weight, power, operating area, and speed comparisons between the 500 nm tiltrotor and the turboshaft and electric 75 nm tiltrotors. Empty weight is used for comparison here to show airframe weight without the fuel differences of the 500 nm and 75 nm missions.

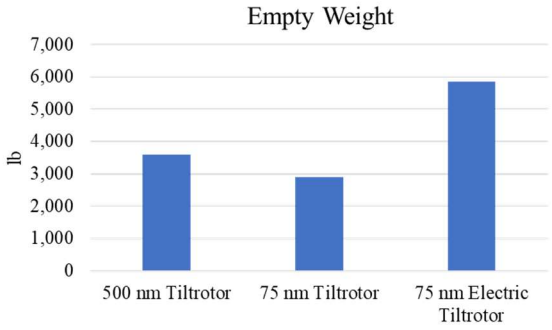

Figure 59. Empty weight comparison

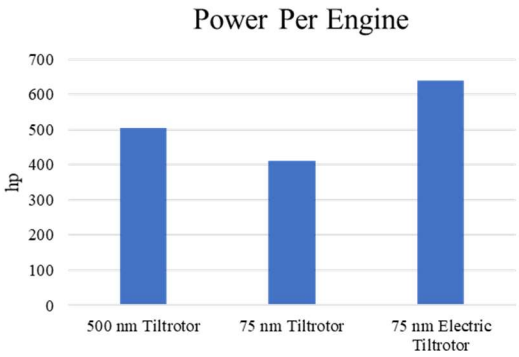

Figure 60. Power comparison

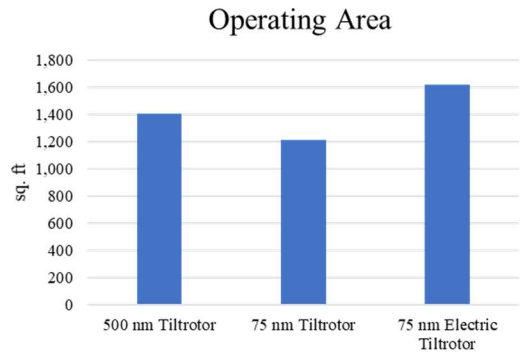

Figure 61. Operating area comparison

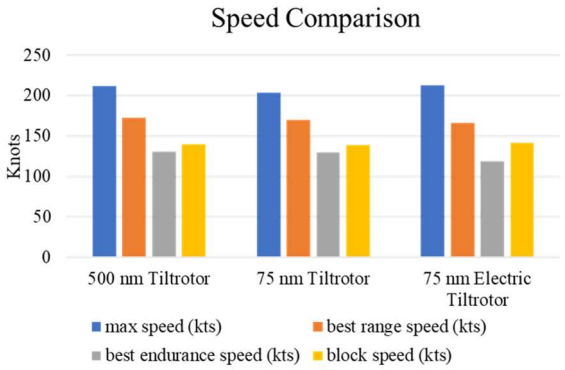

Figure 62. Speed comparison

The 500 nm tiltrotor is sized greater than the 75 nm turboshaft but smaller than the 75 nm electric in weight, power, and size. The speed characteristics are very similar for all the aircraft, giving them all very similar 75 nm mission performance with a block time of about 32 minutes. The larger 500 nm tiltrotor takes 22 more pounds of fuel to fly the mission than the tiltrotor sized for the 75 nm mission, an 11% increase.

The costs in Figure 63-64 follow a similar pattern, increasing per trip cost and aircraft cost levels from the 75 nm turboshaft, but staying below the electric.

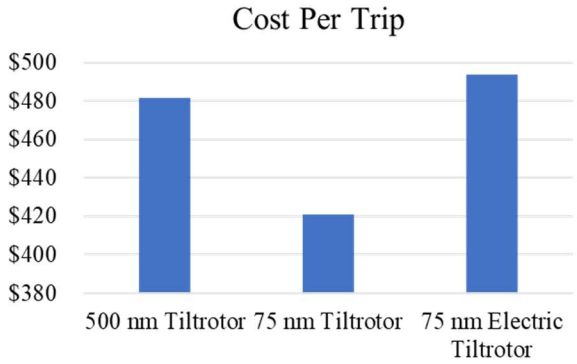

Figure 63. Cost per trip comparison (75 nm mission)

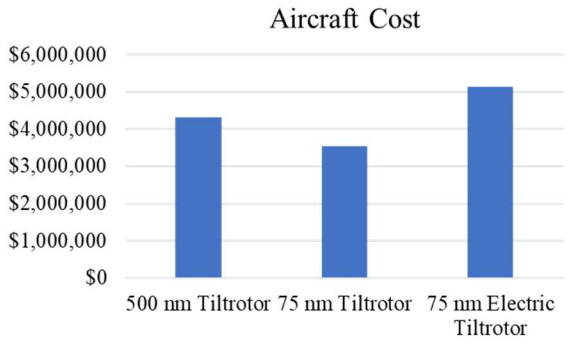

Figure 64. Aircraft cost comparison

A comparison of some of the parameters and the numbers that correspond to the charts are shown in Table 6

Table 6. 500 nm tiltrotor comparison

	500 nm Tiltrotor	75 nm Tiltrotor	75 nm Electric Tiltrotor
Design gross weight (lb)	5,651	4,300	7,053
Diskloading (psf)	11	12	10
Rotor radius (ft)	9.0	7.6	10.6
Rotor chord (ft)	0.74	0.68	0.79
Rotor aspect ratio	12.16	11.15	13.38
Wingloading (psf)	70	60	65
Hover tip speed (ft/s)	550	550	550
Empty weight (lb)	3,592	2,893	5,844
Operating area (sq. ft)	1,403	1,210	1,620
Lock number	8.51	7.95	8.99
Power per engine (hp)	503	411	638
Aircraft cost ($)	4,317,596	3,529,070	5,132,684
Max speed (kts)	212	204	213
Best range speed (kts)	172	170	167
Best endurance speed (kts)	131	129	119
75 nm Mission			
Gross weight (lb)	5020	4300	7053
Cost per trip ($)	482	421	494
Fuel/battery weight (lb)	218	196	1950
Block speed (kts)	140	139	142
Cruise speed (kts)	180	179	174
Block time (min)	32.1	32.3	31.7

FUTURE WORK

Further optimization can be performed on the rotor models for these designs. The design process described in this work optimizes a linear twist and taper. More in-depth study could be done on optimizing a variable twist and taper blade. A two-parameter taper with linear twist would likely improve the rotor performance the most with the least number of design variables, but the level of optimization would increase with increasing number of blade sections with variable twist and taper.

Whirl flutter instability is a type of aeroelastic instability that may affect any aircraft with wing mounted propellers, namely turboprop airplanes and tiltrotors. The rotational motion of the rotor and engine can introduce additional forces and moments that cause the rotor nacelles to move in a circular motion. Whirl flutter has caused crashes of turboprop aircraft in the past, and demonstrating the absence of whirl flutter was a principal objective of the XV-15 aircraft development. For this design to advance in the design process, structural analysis of the wing and nacelle/rotor must be performed, and the wing must be designed to avoid whirl flutter instability modes.

Noise is an important consideration in the design of UAM vehicles. ANOPP2 [23] is an aircraft noise prediction program that can be run with CAMRADII output and is being used to analyze other NASA reference vehicles. These tiltrotors should be analyzed in ANOPP2 and have noise data compared to other reference vehicle configurations and noise annoyance standards.

CONCLUSIONS

Two tiltrotor aircraft were designed for use in Urban Air Mobility using turboshaft and electric propulsion. They were informed by the side-by-side reference vehicle and the High Efficiency Civil Tiltrotor, and represent advanced tiltrotor technology. NDARC was used to size the aircraft to the UAM mission and explore the effects of design changes. CAMRADII was used to determine a higher fidelity rotor model to improve the accuracy of the NDARC calculations. The resultant aircraft were analyzed and compared to other UAM reference vehicles in sizing, cost, and performance. The primary advantage of the tiltrotor vehicles is significantly increased speed, resulting in decreased mission time. The decreased mission time then translates to a lower cost per trip. The speed increase comes with a slight weight, power, and fuel consumption tradeoff, as the tiltrotors are heavier and include more installed power than the side-by-side and quadrotor vehicles, but still lighter and lower power than the lift+cruise. Tiltrotor aircraft appear to be a viable configuration for Urban Air Mobility when speed is a priority and generate a high-performance aircraft solution with manageable tradeoffs.

Author contact: Michael Radotich
michael.t.radotich@nasa.gov

APPENDIX - DRAWINGS

Figure A1: Turboshaft Cruise Mode

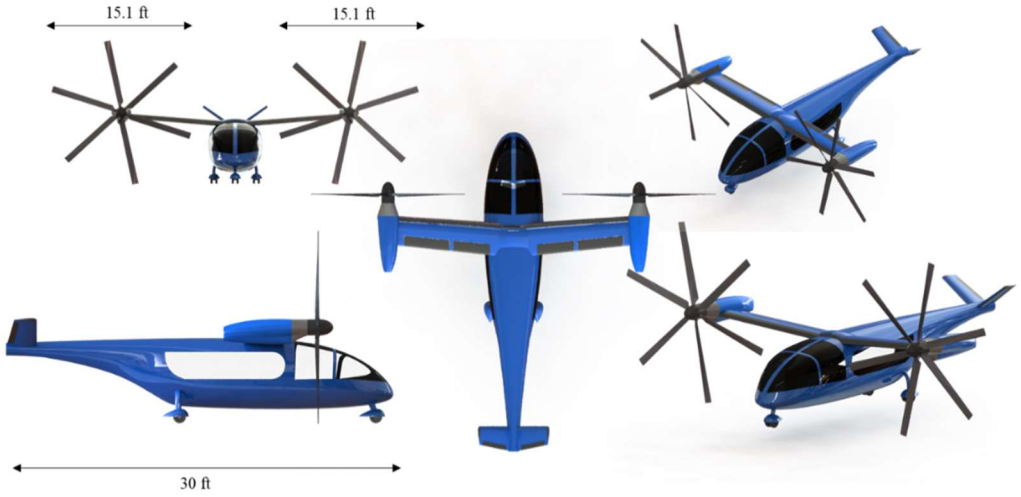

Figure A2: Turboshaft Hover Mode

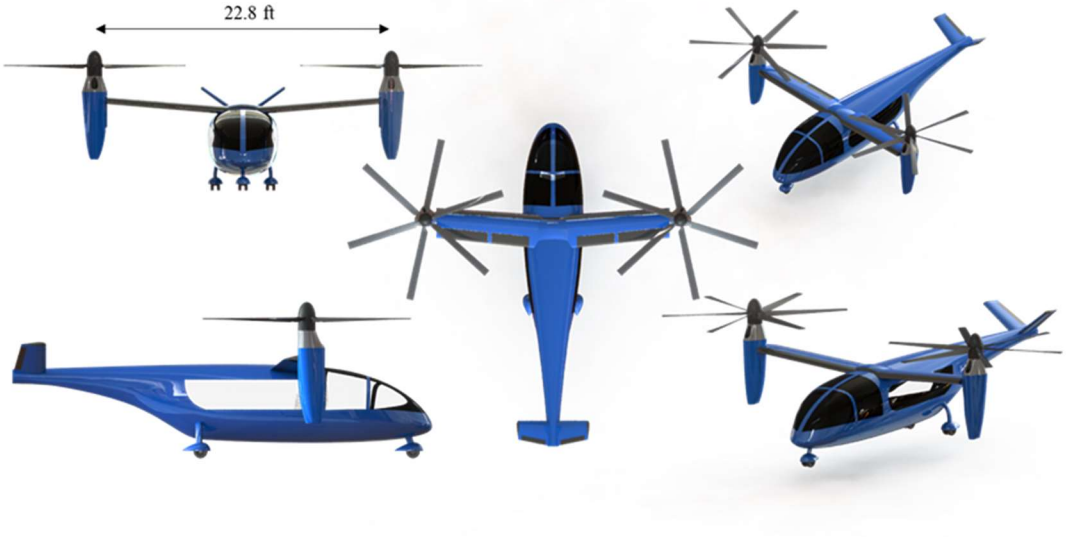

Figure A3: Electric Cruise Mode

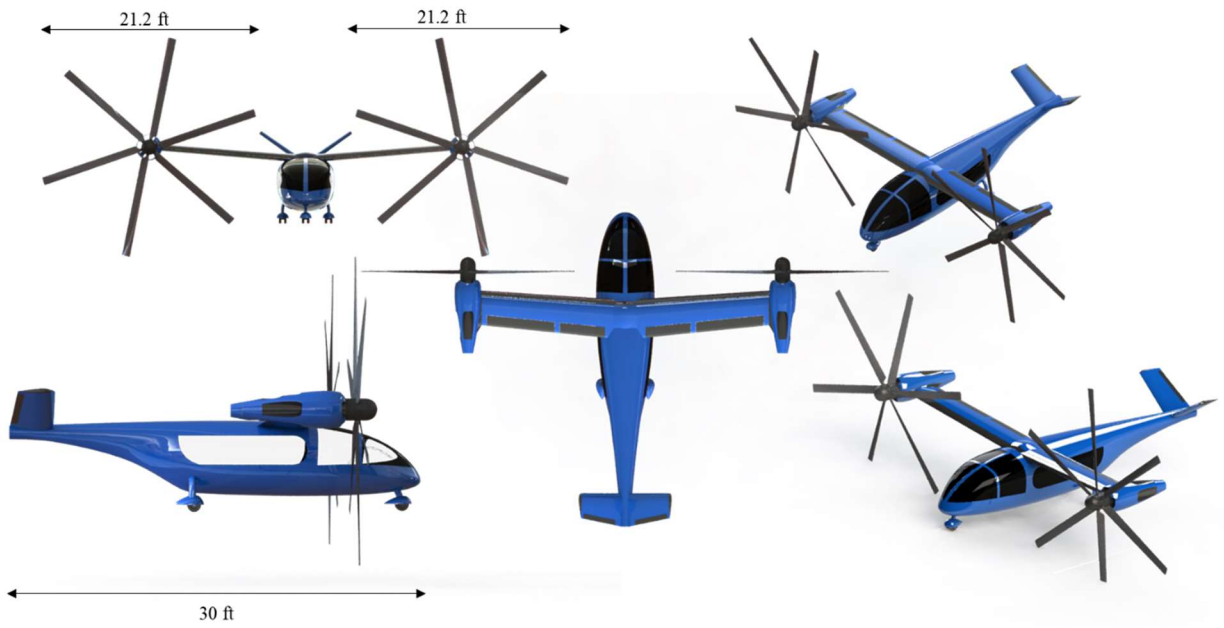

Figure A4: Electric Hover Mode

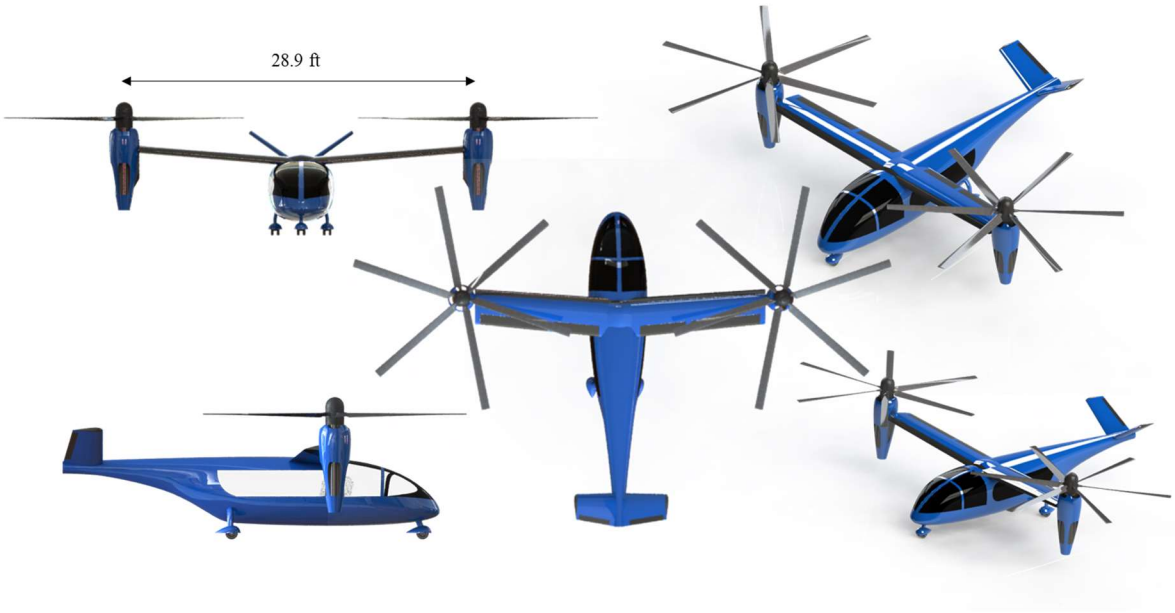

ACKNOWLEDGMENTS

I would like to thank Dr. Wayne Johnson and Chris Silva for their mentorship, guidance, and vast technical knowledge that I have been able to utilize while working on these designs. I would also like to thank Dr. William Warmbrodt for his support of myself and this work.

REFERENCES

[1] J. Holden and N. Goel, "Fast-Forwarding to a Future of On-Demand Urban Air Transportation," pp. 1–98, 2016, [Online]. Available: https://www.uber.com/elevate.pdf.

[2] The Vertical Flight Society, "eVTOL Aircraft Directory," *Electric VTOL News, by the Vertical Flight Society*, 2021. https://evtol.news/aircraft.

[3] C. Silva, W. Johnson, K. R. Antcliff, and M. D. Patterson, "VTOL urban air mobility concept vehicles for technology development," *2018 Aviation Technology, Integration, and Operations Conference*, pp. 1–16, 2018, doi: 10.2514/6.2018-3847.

[4] W. Johnson, C. Silva, and E. Solis, "Concept vehicles for VTOL air taxi operations," *Proc. AHS Int. Tech. Meet. Aeromechanics Des. Transform. Vert. Flight 2018*, 2018.

[5] M. D. Patterson, K. R. Antcliff, and L. W. Kohlman, "A proposed approach to studying urban air mobility missions including an initial exploration of mission requirements," *Annu. Forum Proc. - AHS Int.*, vol. 2018-May, 2018.

[6] C. Bolkcom, "V-22 Osprey Tilt-Rotor Aircraft," 2004.

[7] M. D. Maisel, D. J. Giulianetti, and D. C. Dugan, "The History of The XV-15 Tilt Rotor Research Aircraft: From Concept to Flight," *NASA Spec. Publ. 4517*, p. 194, 2000.

[8] W. Johnson, "NDARC 1.14 - Theory," *Nasa/Tp–2009-215402*, no. April, 2019, [Online]. Available: http://www.scopus.com/inward/record.url?eid=2-s2.0-77953487876&partnerID=40&md5=7e215c2835081968c2107ca6e4cc4787.

[9] C. Silva, W. Johnson, and E. Solis, "Multidisciplinary conceptual design for reduced-emission rotorcraft," *Proc. AHS Int. Tech. Meet. Aeromechanics Des. Transform. Vert. Flight 2018*, 2018.

[10] C. W. Acree and W. Johnson, "Performance, loads and stability of heavy lift tiltrotors," *Am. Helicopter Soc. AHS Vert. Lift Des. Conf.*, vol. 2006, pp. 63–71, 2006.

[11] D. Raymer, *Aircraft Design: A Conceptual Approach*, Sixth Edit. American Institute of Aeronautics and Astronautics, 2018.

[12] W. Johnson, "NDARC - NASA design and analysis of rotorcraft theoretical basis and architecture," *AHS Aeromechanics Specialists Conference 2010*, no. February. pp. 778–803, 2010.

[13] W. Johnson, "NDARC - NASA design and analysis of rotorcraft validation and demonstration," *AHS Aeromechanics Spec. Conf. 2010*, no. April 2010, pp. 804–837, 2010.

[14] C. Silva *et al.*, "The high efficiency tiltrotor as a solution to the needs of a mobile military," *Am. Helicopter Soc. Int. - AHS Spec. Conf. Aeromechanics Des. Vert. Lift 2016*, pp. 273–324, 2016.

[15] A. Chavez, T. Baker, and J. Fetty, "Future Advanced Rotorcraft Drive System (FARDS) full scale gearbox demonstration," *Annu. Forum Proc. - AHS Int.*, no. Reference 2, pp. 2325–2335, 2017.

[16] Y. Mikhaylik, I. Kovalev, L. Liao, M. Laramie, and U. Schoop, "650 Wh / kg , 1400 Wh / L Rechargeable Batteries for New Era of Electrified Mobility," *2018 NASA Aerosp. Batter. Work.*, pp. 1–20, 2018, [Online]. Available: https://www.nasa.gov/sites/default/files/atoms/files/650_whkg_1400_whl_recharg_batt_new_era_elect_mobility_ymikhaylik_0.pdf.

[17] T. Berger, "Karem TR36XP DARPA VTOL X-Plane," *DARPA VTOL X-pl. TR36XP AHS Forum*, pp. 1–19, 2016.

[18] W. Johnson, "Rotorcraft dynamics models for a comprehensive analysis," *Annu. Forum Proc. - Am. Helicopter Soc.*, vol. 1, pp. 452–471, 1998.

[19] C. Acree, H. Yeo, and J. Sinsay, "Performance Optimization of the NASA Large Civil Tiltrotor," *Int. Powered Lift Conf.*, no. June, p. 14, 2008, [Online]. Available: http://oai.dtic.mil/oai/oai?verb=getRecord&metadataPrefix=html&identifier=ADA508826

[20] Dassault Systemes, "SOLIDWORKS." .

[21] J. D. Sinsay, D. M. Hadka, and S. E. Lego, “An integrated design environment for NDARC,” *Am. Helicopter Soc. Int. - AHS Spec. Conf. Aeromechanics Des. Vert. Lift 2016*, vol. 2015, pp. 162–174, 2016.

[22] M. M. M. Monjon and C. M. Freire, “Conceptual design and operating costs evaluation of a 19-seat all-electric aircraft for regional aviation,” *AIAA Propuls. Energy 2020 Forum*, pp. 1–16, 2020, doi: 10.2514/6.2020-3591.

[23] L. V. Lopes and C. L. Burley, “Design of the next generation aircraft noise prediction program: ANOPP2,” *17th AIAA/CEAS Aeroacoustics Conf. 2011 (32nd AIAA Aeroacoustics Conf.*, no. November, 2011, doi: 10.2514/6.2011-2854.